Electronic Supplementary Material (ESI) for ChemComm.

Supporting Information

Visible light-mediated C(sp^3)-H bond functionalization inside an all-organic nanocavity

Debojyoti Roy, Sunandita Paul and Jyotishman Dasgupta *

1. Materials and Methods.....4-5

2. Supplementary Figures.....6-39

S1: ^{1}H NMR spectra of DB.2PF$_6$.

S2: ^{1}H NMR spectra of ExBox.4PF$_6$ synthesized in Microwave chamber.

S3: ^{1}H NMR spectra of 1-MePy in ExBox.4PF$_6$

S4: ^{1}H NMR spectra of 1-MePy in ExBox.4PF$_6$ showing peak area integration

S5: ^{1}H NMR spectra of 9-MA in ExBox.4PF$_6$ showing peak area integration

S6: ^{1}H NMR spectra of 9-MA in ExBox.4PF$_6$

S7: ^{1}H NMR spectra of 1-MeNap in ExBox.4PF$_6$

S8: ^{1}H NMR spectra showing displacement of 1MeNap from ExBox after Pyrene addition

S9: Uv-Vis absorption titration of 1MePy in ExBox and calculation of binding constant

S10: ^{1}H NMR spectra of photoproduct of 1-MePy in ExBox.4PF$_6$ after 460 nm LED illumination

S11: GCMS trace of photoproduct of 1-MeNap in ExBox.4PF$_6$ after 460 nm LED illumination

S12: GCMS trace of photoproduct of 9-MA in ExBox.4PF$_6$ after 520 nm LED illumination

S13: ^{1}H NMR spectra of photoproduct of 9-MA in ExBox.4PF$_6$ after 520 nm LED illumination

S14: GCMS trace of photoreaction 9-MA under inert condition after 520 nm LED illumination

S15: GCMS trace of photoreaction of 9-MA, 1-MeNap, Toluene without cavity

S16: GCMS trace of reaction of 9-MA, 1-MeNap, Toluene without light

S17: GCMS trace of photoreaction of 1-MeNap, Toluene with DB.2PF$_6$

S18: GCMS trace of photoreaction of Cumene in ExBox with 400 nm LED

S19: GCMS trace of photoproduct of Toluene in ExBox.4PF$_6$ after 400 nm LED illumination

S20: GCMS trace of photoproduct of 2-MeThiophene in ExBox.4PF$_6$ after 400 nm LED illumination

S21: GCMS trace of photoreaction of Ethyl, Propyl and Butylbenzene in ExBox after 400 nm LED illumination

S22: Spectral shift in NIR region for 1-MePy, 9-MA, 1-MeNap in ExBox.4PF$_6$ from Transient absorption spectroscopy.

S23: SVD of Transient absorption data of 1-MePy in ExBox.4PF$_6$ after addition of 20 % water in ACN

S24: SVD of Transient absorption data of 9-MA in ExBox.4PF$_6$ in visible region.

S25: SVD of Transient absorption data of 1-MeNap in ExBox.4PF$_6$ in visible region.

S26: Normalized Single wavelength kinetics of 1-MePy in ExBox.4PF$_6$ with and without water addition from TA data.

S27: Computed transitions for 1-MePy radical cation using TD-DFT

S28: Computed transitions for 1-MePy neutral radical using TD-DFT

S29: Primary KIE measurements with 9-MA and d_{12}-9-MA in ExBox.4PF_6

S30: Wavelength dependant Transient absorption measurements for 9-MA and 9-MA in ExBox.4PF_6

S31: GCMS trace of photoproducts of 1-MeNap in ExBox.4PF_6 in different ACN: Water Ratio

S32: Steady state absorption of ExBox, 1-MePy and 1-MePy in ExBox

S33: Steady state absorption of ExBox, 1-MeNap and 1-MeNap in ExBox

S34: Normalized Absorption and Emission spectra of ExBox.4PF_6

S35: ESIMS of ExBox.4PF_6

S36: ^{1}H NMR spectra during photoreaction of 1-MePy in ExBox.4PF_6 after 460 nm LED illumination

S37: ^{1}H NMR spectra of control reaction of 1-MePy after 460 nm LED illumination

S38: Normalized Single wavelength kinetics of 1-MePy in ExBox.4PF_6 at 461 nm

S39: Normalized Single wavelength kinetics of 1-MePy in ExBox.4PF_6 at 1140 nm

S40: Population analysis of 1-MePy in ExBox.4PF_6 after SVD

S41: Example of Photoreaction protocol of 9-MA in ExBox.4PF_6 with 520 nm LED

S42: SVD of Transient absorption data of 1-MePy in ExBox.4PF_6 after addition of 20 % D_2O in CAN

S43: SVD of Transient absorption data of 1-MeNap in ExBox.4PF_6 in CD_3CN.

S44: UV-Vis titration of 1MePy in Acetonitrile without ExBox addition.

S45: ^{1}H NMR spectra of 1-MeNap in ExBox.4PF_6 showing peak area integration

S46: Single crystal x-ray structure of 9-MA in ExBox.4PF_6

S47: HOMO-LUMO electron densities of 9-MA in ExBox.4PF_6

Supporting Table 1 –5: Output details of DFT calculations

3. References..... 41

Materials and Methods:

Chemicals Used: Ex-Bipy (1,4-Di(4-pyridyl)benzene), 1-Methylpyrene (1-MePy) from TCI Chemicals Pvt. Ltd .α,ά Di-bromo-p-xylene, Pyrene, 1-Methylnaphthalene(1-MeNap), 9-Methylanthracene (9-MA) , Toluene ,2-Methylthiophene purchased from Sigma-Aldrich respectively. All reagents were used as supplied for the reactions.

Microwave synthesis: All synthesis was carried out in a microwave chamber (ETHOS, Nano catalysis lab, TIFR). The ramp profile was given as 10 min delay to reach to 80°C from room temperature and then up to 2 hours 80°C was maintained.

NMR Characterization: ^{1}H-NMR spectra were recorded on Varian-600 (600 MHz) spectrometer.

Steady State Absorption and Emission: Steady state absorption measurements were performed using a commercial JASCO V-670 spectrophotometer. Steady state emission measurements were done in Flourolog-3 (Horiba Jobin Yvon Inc) spectrofluorometer with Xe lamp as excitation source and PMT detector.

Ultrafast Transient Absorption Spectroscopy: All time-resolved measurements were done using transient absorption spectrometer. Femtosecond laser pulses were generated in the oscillator (Coherent Micra-5 Mode-locked Ti: sapphire Laser system) with bandwidth of ~100 nm at 80 MHz repetition rate. The laser pulses were amplified in Coherent Legend Elite Ultrafast Amplifier Laser system to get ~30 fs/3.5 mJ with repetition rate of 1 kHz and bandwidth of ~65 nm. The amplifier output is divided into two parts to generate pump and probe pulses. For 400 nm pump pulse, the amplifier output was focused to a BBO crystal to generate frequency doubled output of the fundamental 800 nm beam. For 520 nm pump pulse, the amplifier output was directed to an optical parametric amplifier (Coherent OPeraASolo Ultrafast Optical Parametric Amplifier system). The white-light probe continuum (420−1400 nm) was generated by focusing amplified output on a 2-mm thick sapphire, which is then directed to a multichannel detector procured from Ultrafast Systems. The pump and probe pulses were temporally and spatially overlapped within the sample. All the measurements were done in 1-mm flow cuvette with a peristaltic pump to attain flow rates that minimize the photo degradation of the samples. The temporal resolution obtained in our transient absorption set up was ~ 100 fs.

Kinetic Data Fitting Procedure: Single wavelength kinetic fits for transient absorption was fitted using multi-exponential decay constants in convolution with the respective instrument response function (IRF). It was done in Igor Pro5 Wavemetrics software to get the lifetime and amplitude of each decay component. The equation used was:

$$y = A_0 + \Sigma_i A_i \exp(-t/\tau_i)$$

Global Analysis of TA data: Global analysis of the TA data was done using Glotaran 1.5.1 software. Single value decomposition was done to obtain the Evolution associated spectra (EAS) and their corresponding lifetimes.

Synthesis of ExBox.4PF_6:

Step1: The ExBox cavity was synthesized in 2-steps as described below. The first step was nucleophilic displacement reaction between α, ά di-bromo-p-xylene, Ex-Bipy, followed by an anion exchange to give DB·2PF_6 (scheme 1). The reaction was kept on stirring for two days as per the reported protocol[1]. The obtained product material was characterized by ^{1}H NMR in CD_3CN. Figure 1 shows the recorded NMR spectra of DB·2PF_6 in CD_3CN. δ_H 8.86 ppm (J = 6.9 Hz, 4H), 8.36 ppm (J = 6.9 Hz, 4H), 8.14 ppm (s, 4H), 7.56 ppm (J = 8.2 Hz, 4H), 7.50 ppm (J = 8.2 Hz, 4H), 5.78 ppm (s, 4H), 4.63 ppm (s, 4H).

Step2: A vast range of organic synthesis like transition metal mediated C-C coupling, nucleophilic substitutions, Diels-Alder cycloadditions can be carried out inside a microwave chamber, resulting in better yields with very short reaction time. This strategy catalyzes reactions in many cases. Taking inspiration from these efforts, the final step of the synthesis was tried in microwave chamber rather than in oil bath for 17 days in the presence of a template (pyrene) to give ExBox.4PF_6 as prescribed in published literature[4]. A quick check told us that carrying out the reaction at 80˚C leads to the synthesis of $ExBox^{4+}$ using Tetrabutylammonium Iodide takes around 18 hours for completion. To do it much more efficiently we tried the synthesis in microwave chamber, and got the desired product within 2 hours at 80˚C. This led to the reduction in time from 17 days to 2 hours for the second step. After the successful workup steps, we got crude material with 34 % yield. The material was characterized by ^{1}H NMR in CD_3CN shown in Figure 2. δ_H 8.78 ppm (J = 6.4 Hz, 8H, H_α), 8.18 ppm (J = 6.4 Hz, 8H, H_β), 7.94 ppm (s, 8H, H_γ), 7.62 ppm (s, 8H, Ph), 5.7 ppm (s, 8H, CH_2).

Sample preparation: Solid cage powder was weighed and dissolved in acetonitrile to prepare a 2.5 mM solution. To make a solution of host-guest complex, 3-4 equivalents of solid/liquid guest were added to the cage solution, and stirred in dark for 1 hour in a glass vial at room temperature and ambient pressure. The solution was then syringe filtered to remove the excess guests in solution (if any).

Crystallization: Slow vapor diffusion of iPr_2O into the solution of 9-MA and ExBox.4PF_6 in Acetonitrile yielded orange-red single crystals within 2 days.

Computational details: DFT calculations are performed in the Gaussian 09 program[2]. All the ground state structures are optimized and the optimized geometries of the molecules are confirmed to have

zero imaginary frequencies from vibrational analysis. Using these structures as starting points the absorption wavelengths and oscillator strengths were calculated by TD-DFT formalism[3].

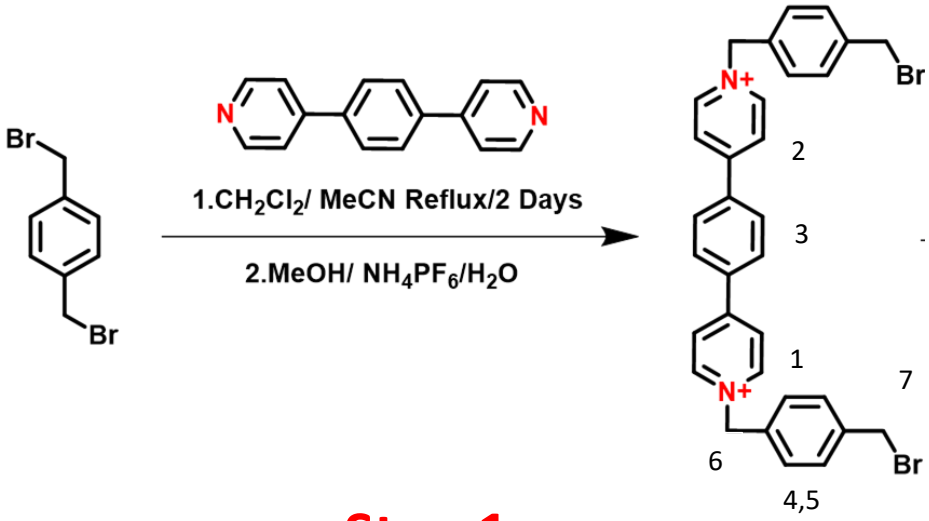

Step 1

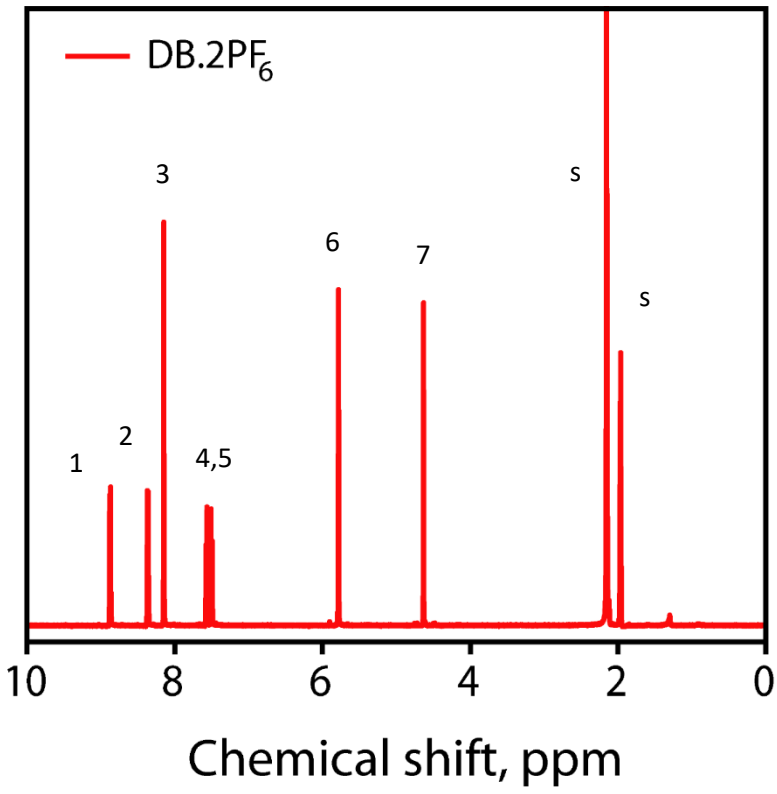

Figure S1. ^{1}H NMR spectra of DB.2PF_6 in CD_3CN. S denotes NMR solvent impurities.

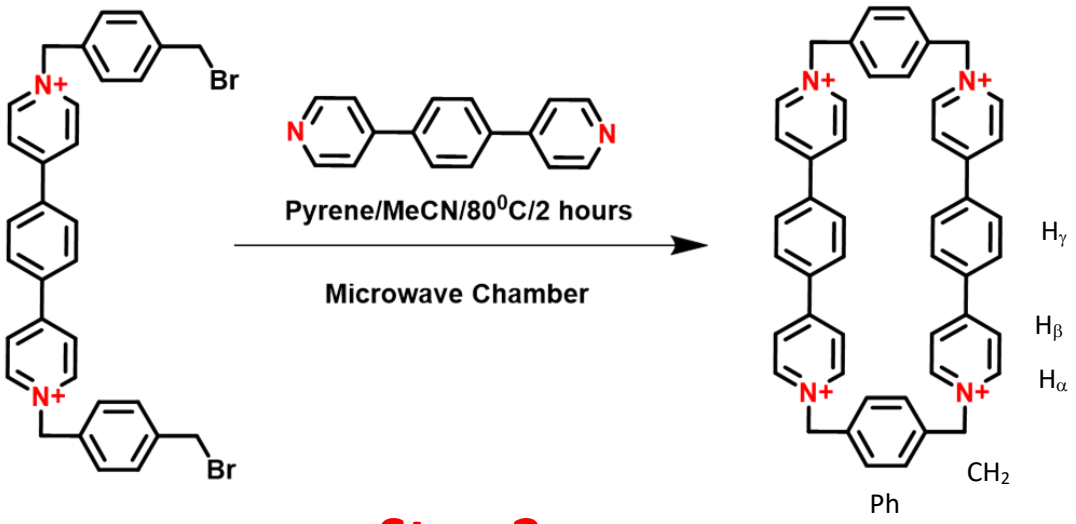

Step 2

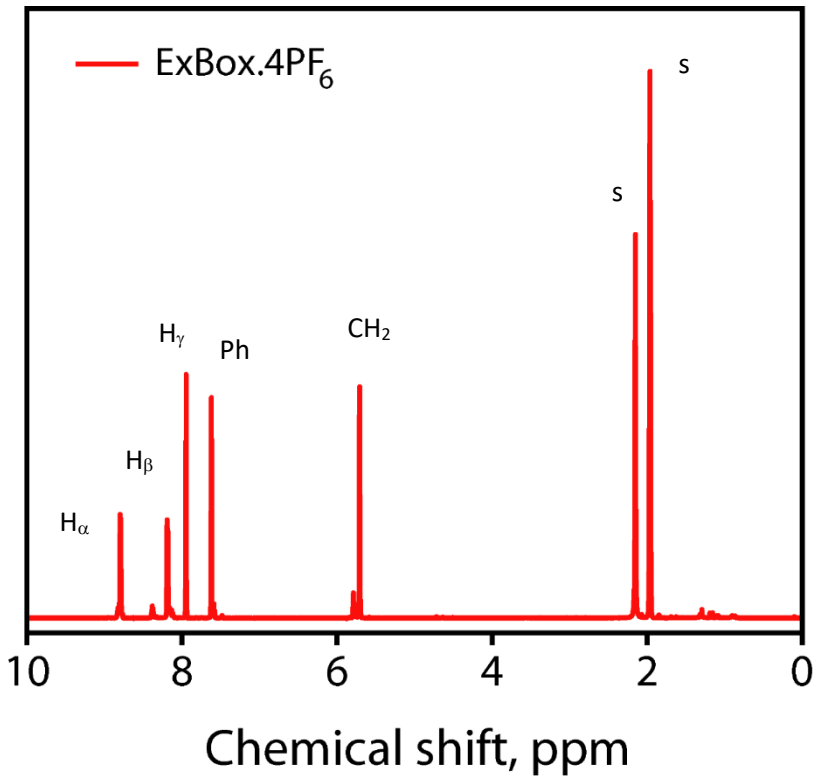

Figure S2. ^{1}H NMR spectra of ExBox.4PF$_6$ in CD_3CN. S denotes NMR solvent impurities.

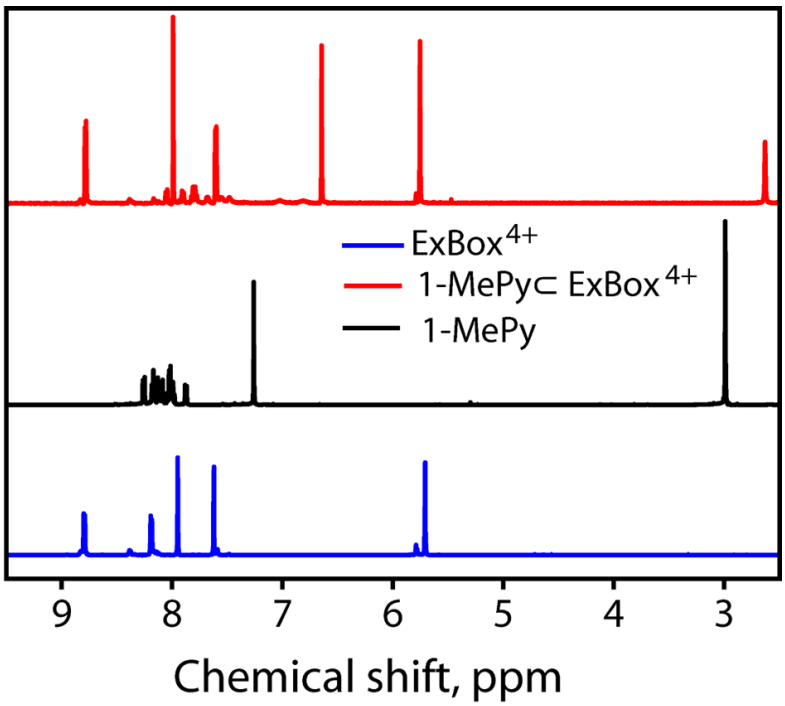

Figure S3. ^{1}H NMR spectra of ExBox^{4+}, 1-MePy and 1-MePy ⊂ ExBox^{4+} in CD_3CN. Up field shift of guest molecule peaks after incarceration shown in red trace.

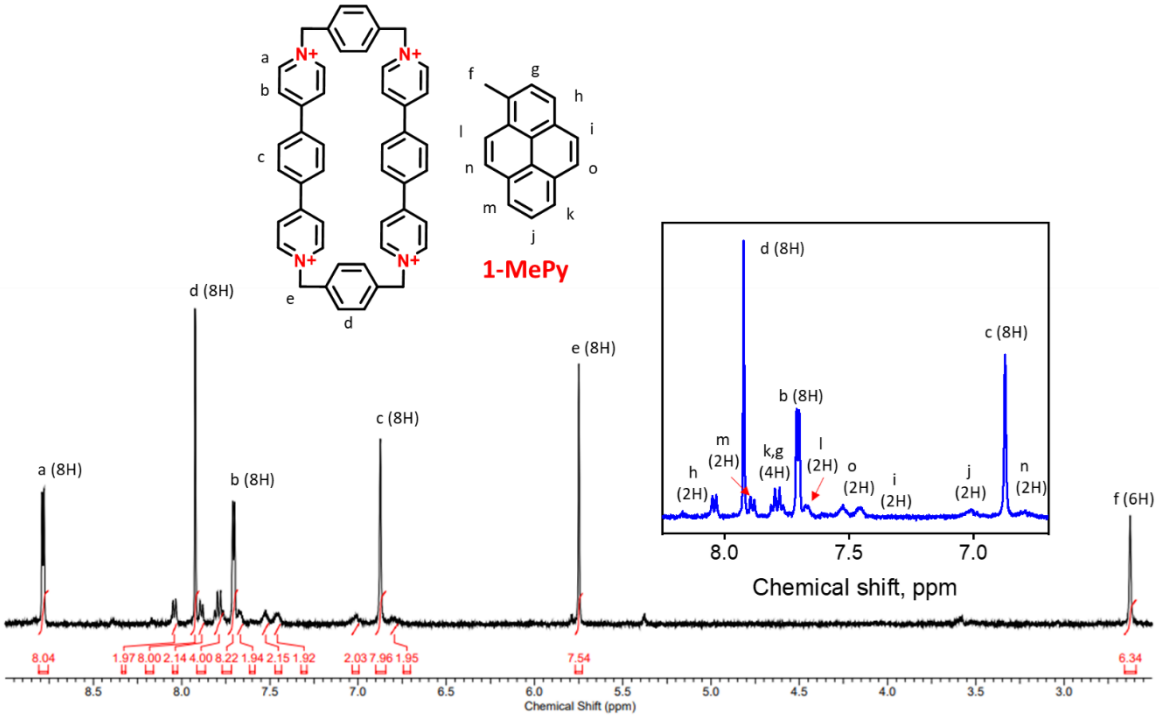

Figure S4. ^{1}H NMR spectra of 1MePy ⊂ ExBox host-guest complex in CD3CN, 600 MHz showing peak area integrations.

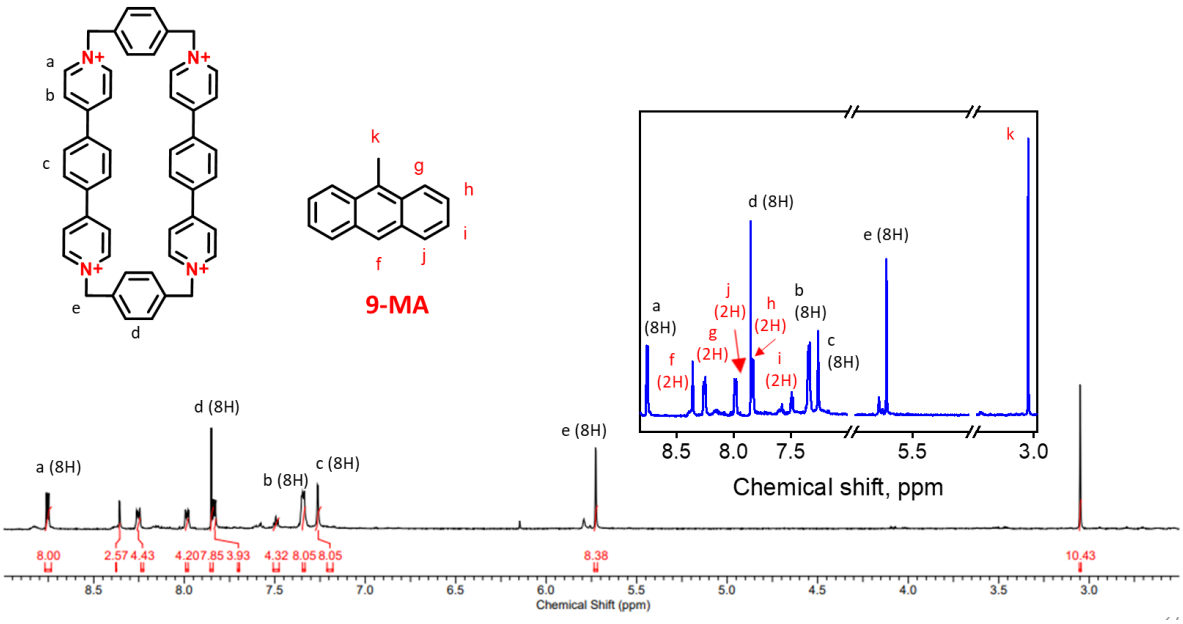

Figure S5. ^{1}H NMR spectra of 9-MA ⊂ ExBox host-guest complex in CD3CN, 600 MHz showing peak area integrations.

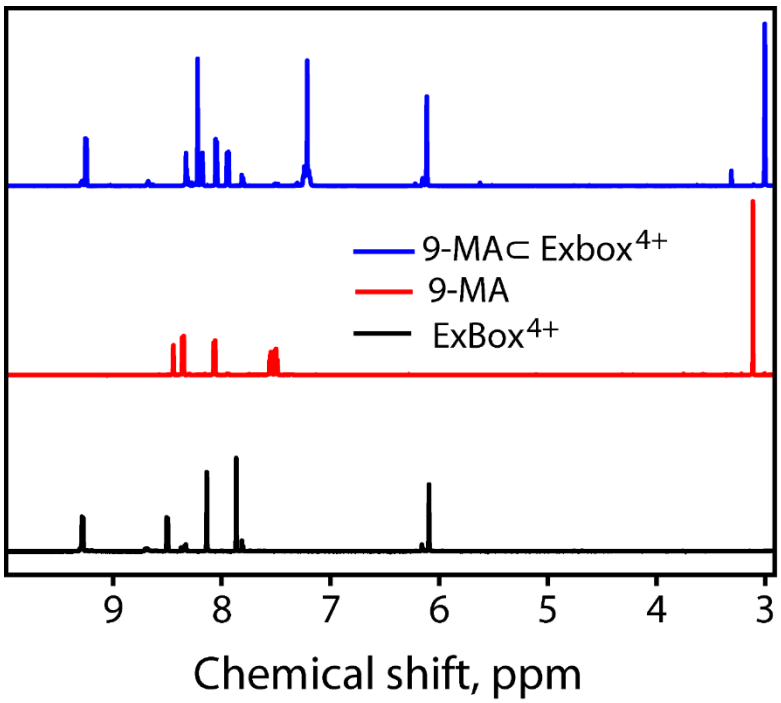

Figure S6. ^{1}H NMR spectra of ExBox^{4+}, 9-MA and 9-MA ⊂ ExBox^{4+} in CD_3COCD_3. Up field shift of guest molecule peaks after incarceration shown in blue trace.

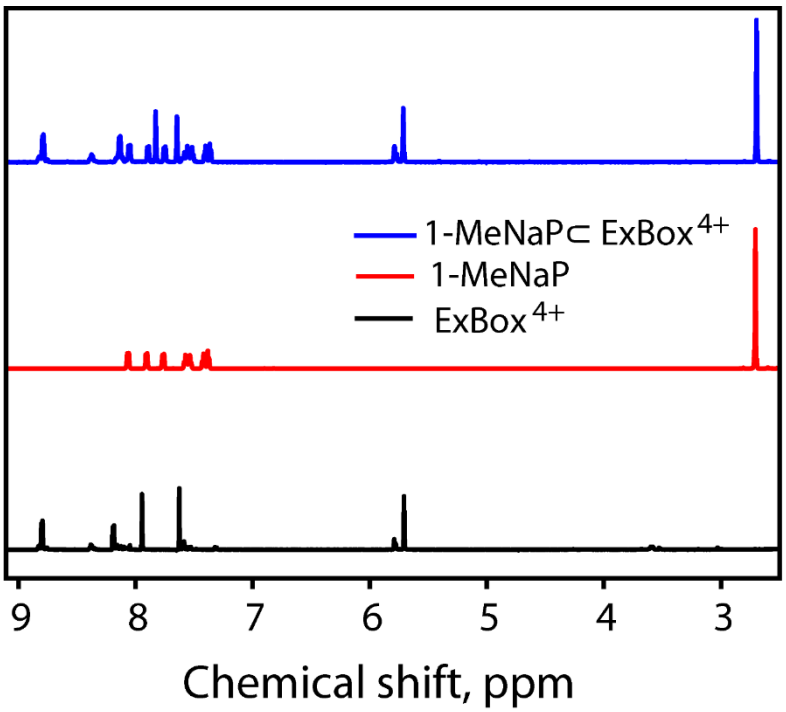

Figure S7. ^{1}H NMR spectra of ExBox^{4+}, 1-MeNap and 1-MeNap ⊂ ExBox^{4+} in CD_3CN. Up field shift of guest molecule peaks after incarceration shown in blue trace.

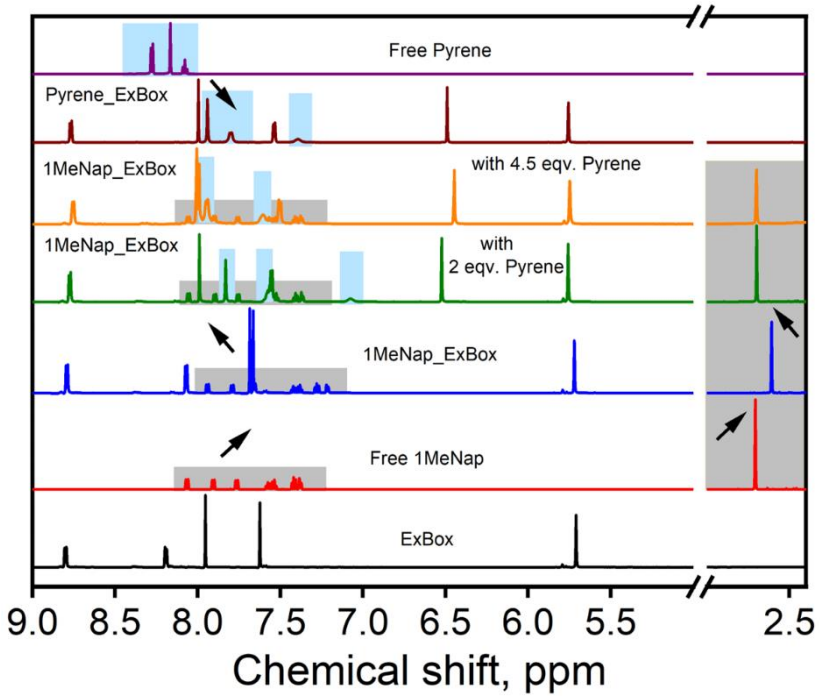

Figure S8. ^{1}H NMR spectra showing replacement of 1MeNap guest from the cavity after addition of Pyrene.

Model for binding of guest derivatives to Host molecule:

The concentration of Host-Guest bound species could be defined as the product of free species concentration with their binding constants

$[HG] = K_1[H][G]$

$[HG_2] = K_2\,[HG][G] = K_2(K_1[H][G])\,[G] = K_1K_2[H][G]^2$

$[HG_N] = K_1K_2\ldots\ldots\ldots K_N[H][G]^N$

Total Host Concentration = Total bound+ Total free=($[HG]+[HG_2]+\ldots\ldots\ldots\ldots+[HG_i]$) +($[H]$)

n = moles of bound Host/moles of total Host

$n = [HG]+[HG_2]+\ldots\ldots\ldots\ldots+[HG_i]/[H]+[HG]+[HG2]+\ldots\ldots\ldots\ldots+[HG_i]$

$n = K_1[H][G] + K_1K_2[H][G]^2 + K_1K_2K_3[H][G]^3+\ldots\ldots+ K_1K_2\ldots\ldots\ldots K_N[H][G]^N/ [H]+ K_1[H][G] + K_1K_2[H][G]^2+ K_1K_2K_3[H][G]^3+\ldots\ldots\ldots + K_1K_2\ldots\ldots\ldots K_N[H][G]^N$

$n=K_1[G]+K_1K_2[G]^2+K_1K_2K_3[G]^3+\cdots K_1K_2K_3\ldots K_M[G]^M/1+K_1[G]+K_1K_2[G]^2+K_1K_2K_3[G]^3+\cdots K_1K_2K_3\ldots K_M[G]^M\ \cdots$

For n=2 we can write

$n= K_1[G]+ K_1K_2[G]^2/\ 1+ K_1[G]+ K_1K_2[G]^2$

where, K_1, K_2, are the binding constants for all corresponding binding steps, n is the fraction of Host bound, and [G] is the concentration of added Guest.

We *plot Normalized Absorbace vs [G] and fit it with the above-mentioned equation to get the individual binding constant values.*

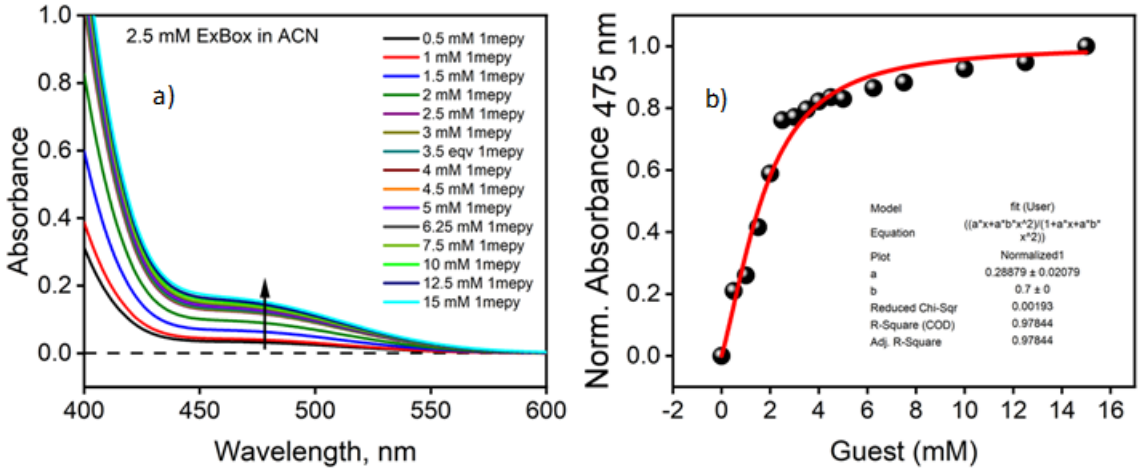

Figure S9. (a) Uv-Vis titration of 1MePy ⊂ ExBox (2.5 mM) host-guest complex. (b) Fitting curve of change in absorbance intensity of CT transitions (at 475 nm) with guest concentrations.

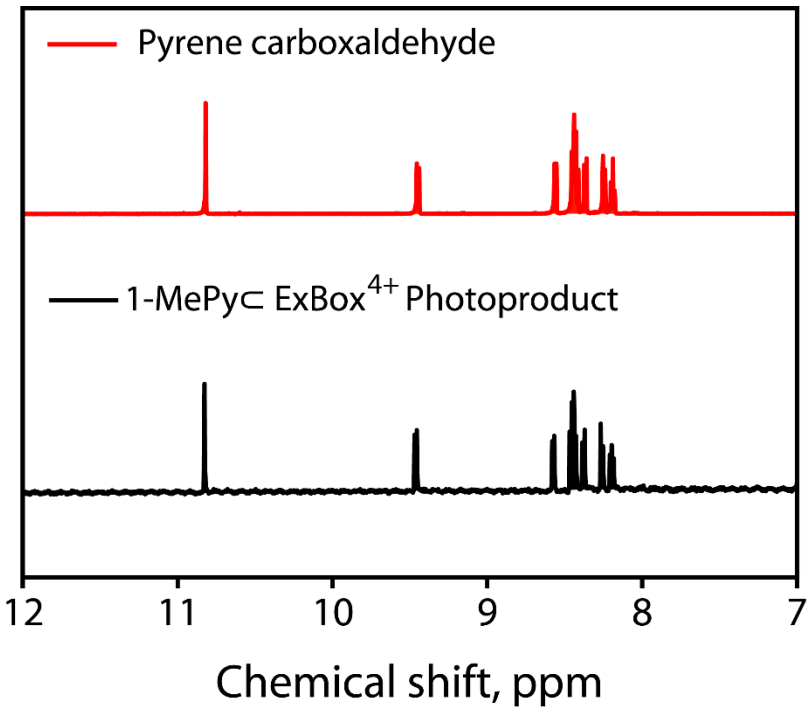

Figure S10. ^{1}H NMR trace photoreactions of 1-MePy ⊂ ExBox^{4+} with 460 nm LED after TLC separation and compared with Pyrene carboxaldehyde in CD_3CN.

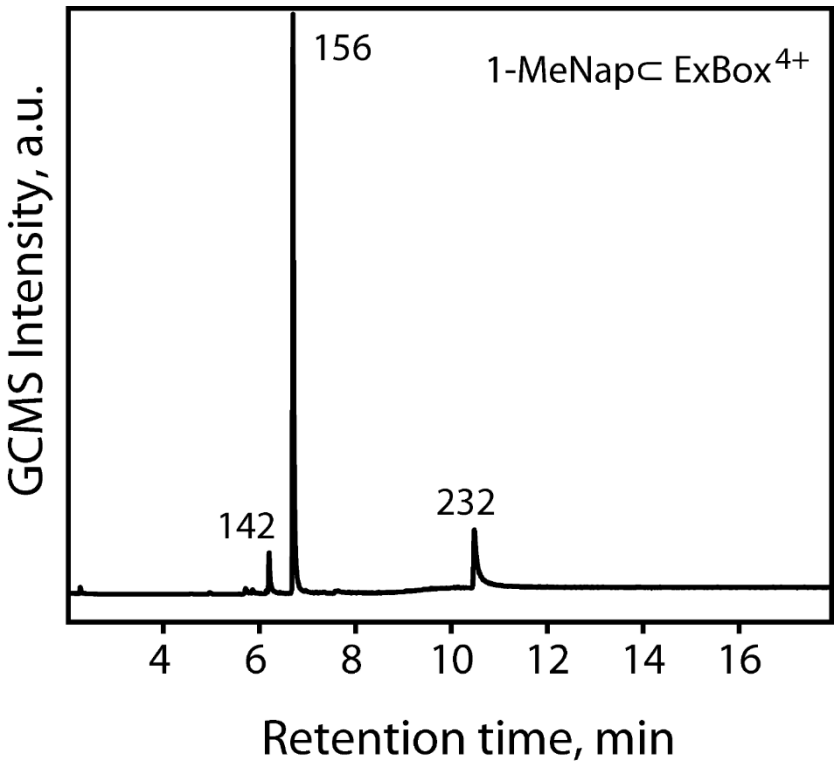

Figure S11. GCMS traces of photoproducts of 1-Menap⊂ ExBox^{4+} in CH_3CN. m/z= 232 corresponds to ExBipy unit from ExBox^{4+} cavity.

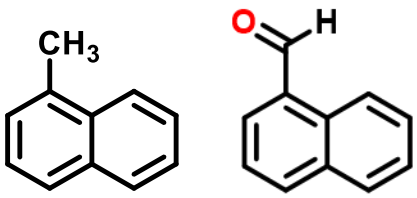

142 156

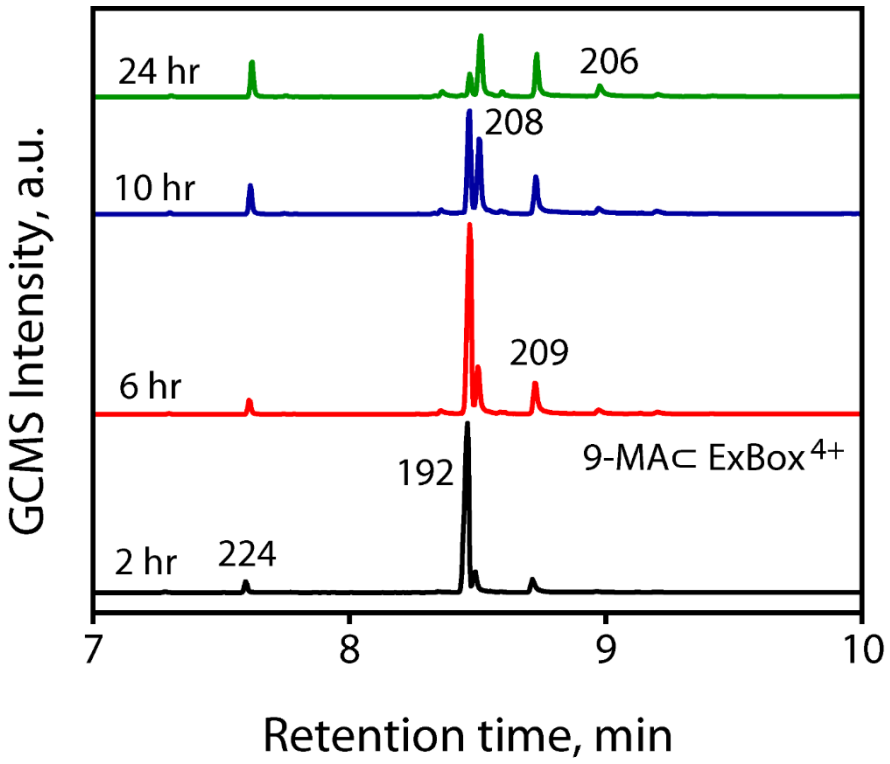

Figure S12. GCMS traces of photoproducts of 9-MA⊂ ExBox^{4+} in CH_3CN. RT (min) = 7.61 and 8.73 corresponds to hydroxylated product (m/z = 226).

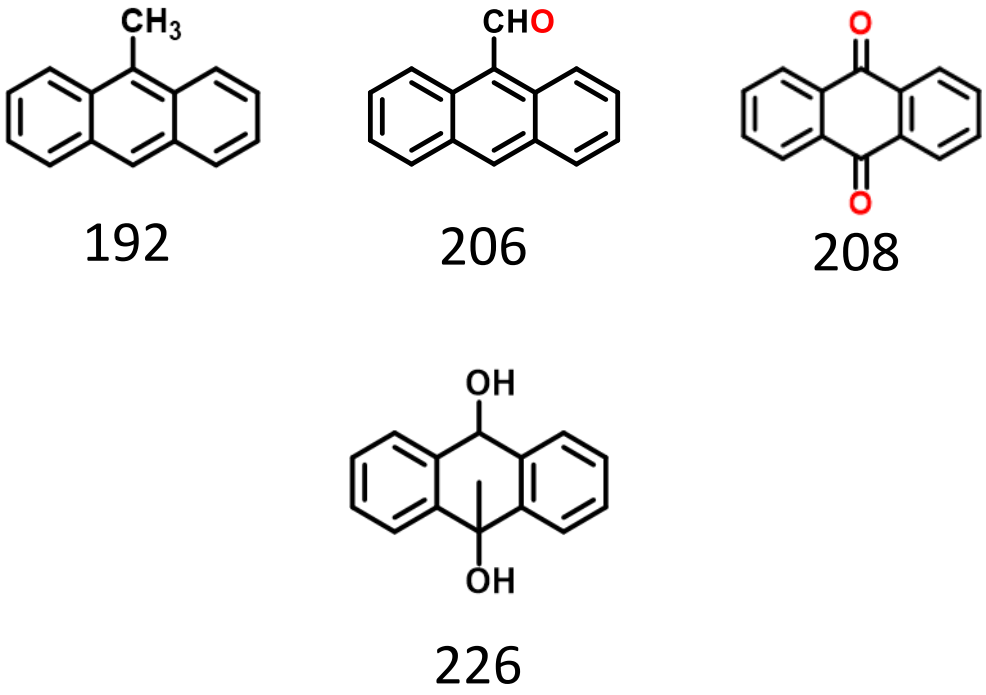

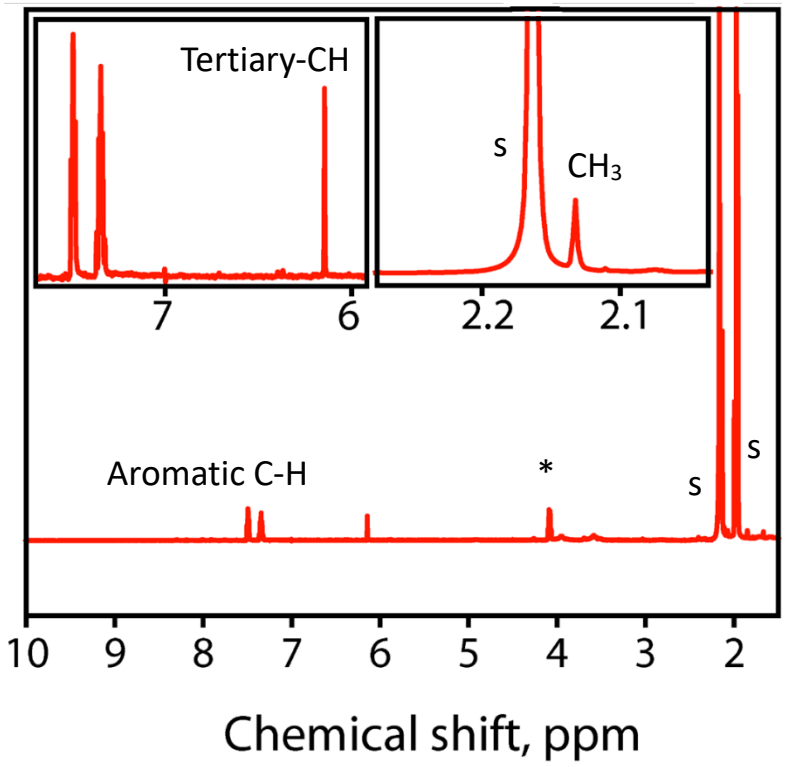

Figure S13. ^{1}H NMR trace of photoproduct of 9-MA⊂ ExBox^{4+}. S denotes NMR solvent impurity and * denotes impurity from Ethyl acetate used for chromatographic separation.

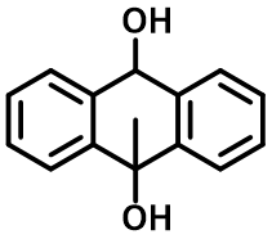

m/z = 226

(From LCMS direct injection)

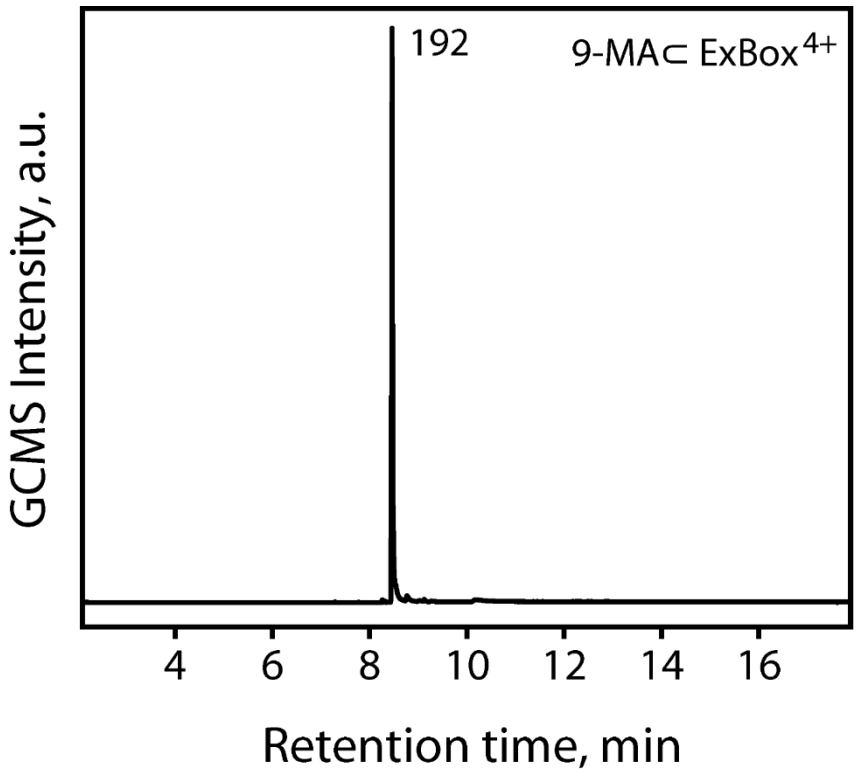

Figure S14. GCMS traces of photoproducts of 9-MA⊂ ExBox^{4+} in CH_3CN under inert conditions.

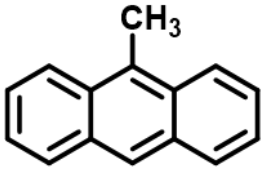

192

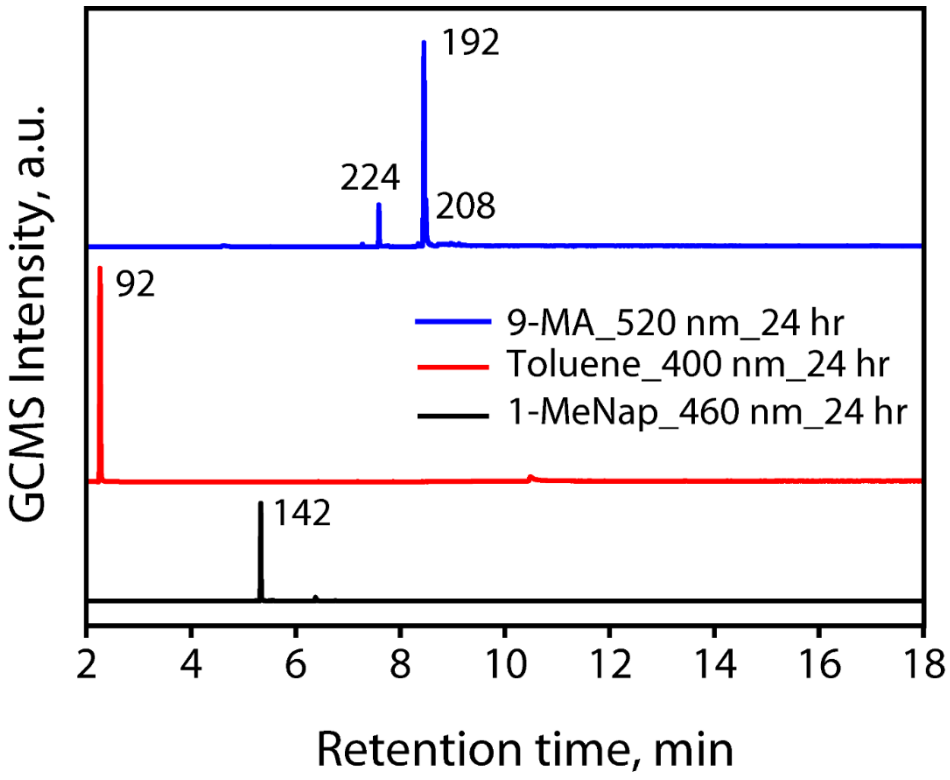

Figure S15. GCMS traces of photoproducts of 1-MeNap. 9-MA and Toluene in CH_3CN.

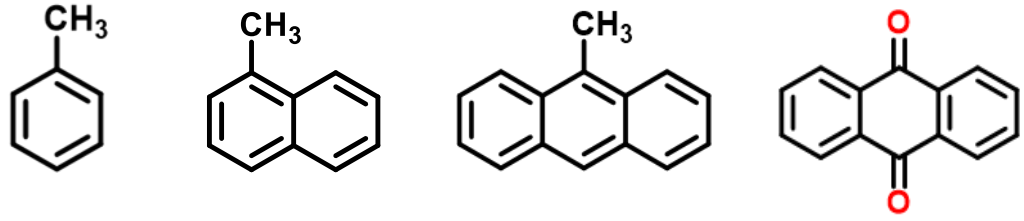

92 142 192 208

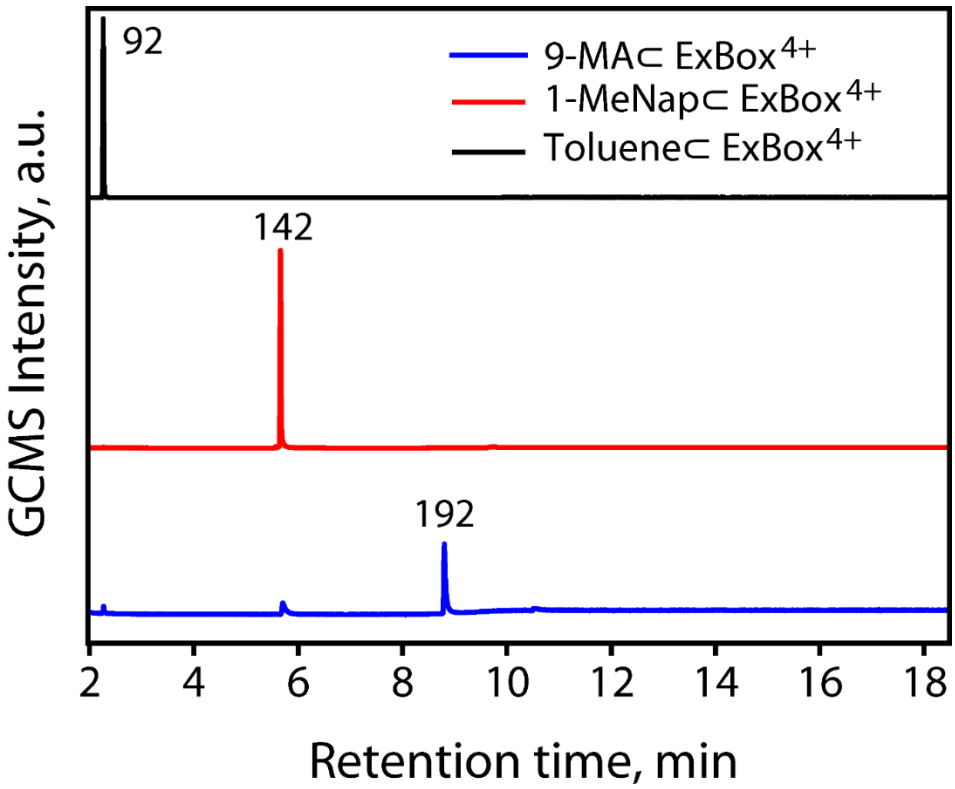

Figure S16. GCMS traces of reactions of 1-MeNap⊂ ExBox^{4+}, 9-MA⊂ ExBox^{4+} and Toluene⊂ ExBox^{4+} in absence of light.

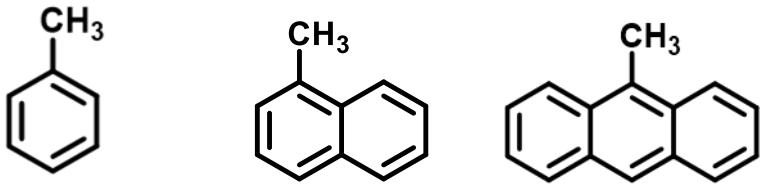

92 142 192

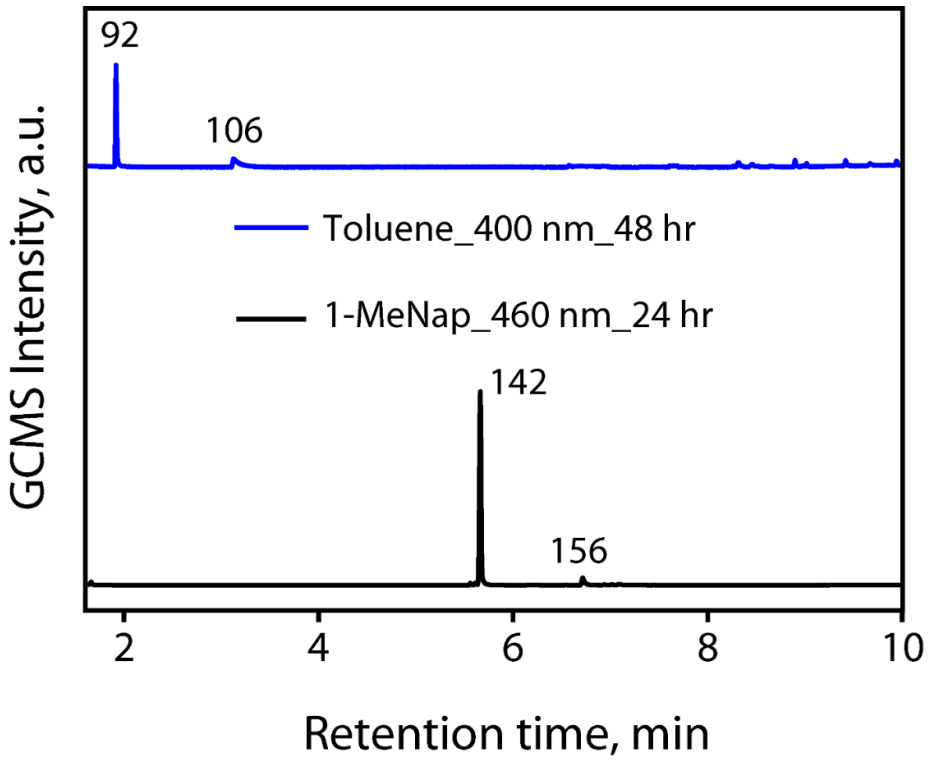

Figure S17. GCMS traces of photoproducts of 1-MeNap. Toluene in presence of DB.2PF_6 in CH_3CN.

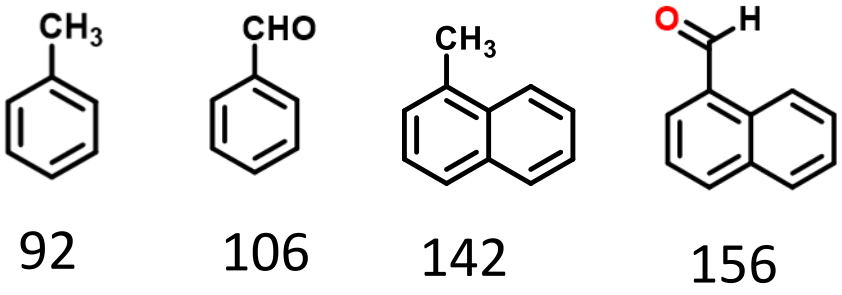

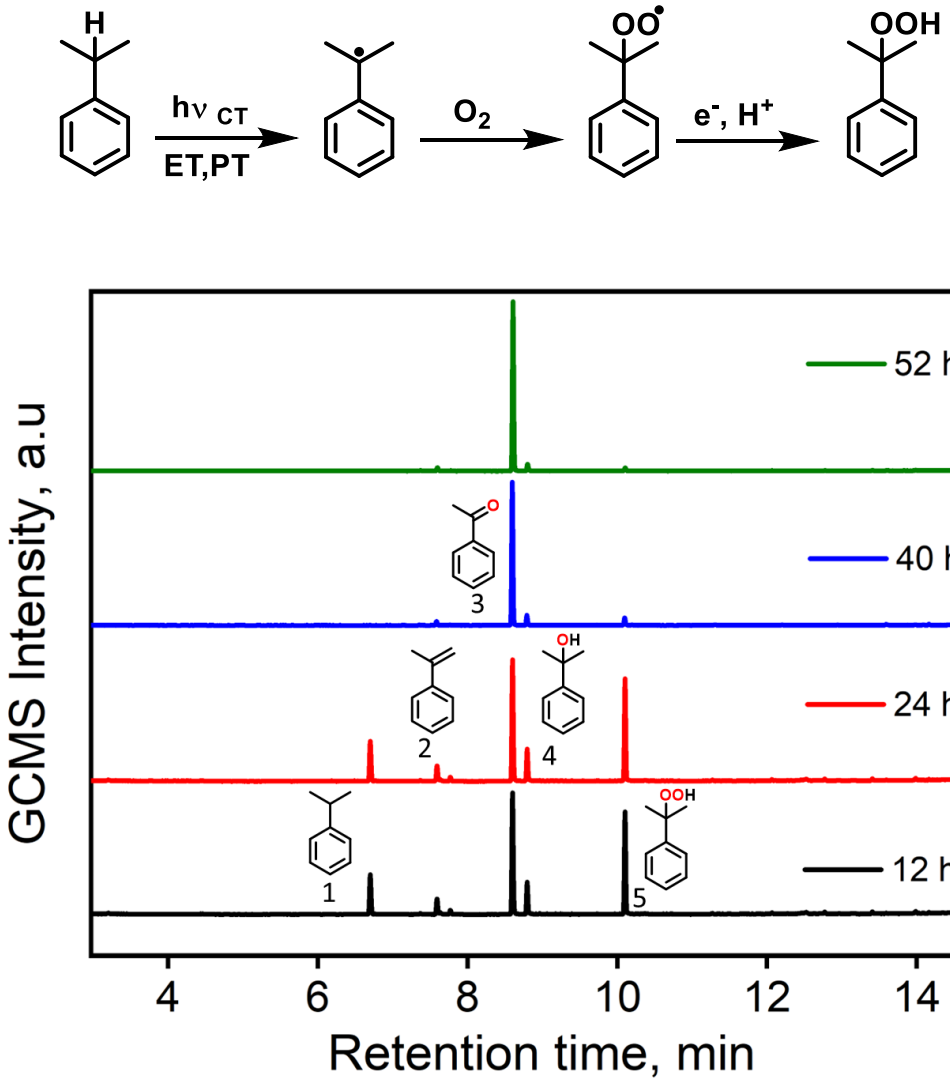

Time (hr)	1	2	3	4	5
12	14.08	5.02	38.86	9.89	32.14
24	9.8	4.48	48.98	10.95	25.79
40	0	2.59	86.32	6.42	4.68
52	0	2	91.90	4.17	1.93

Figure S18. GCMS Traces and Percentage of Photoproducts of Cumene oxidation inside ExBox.

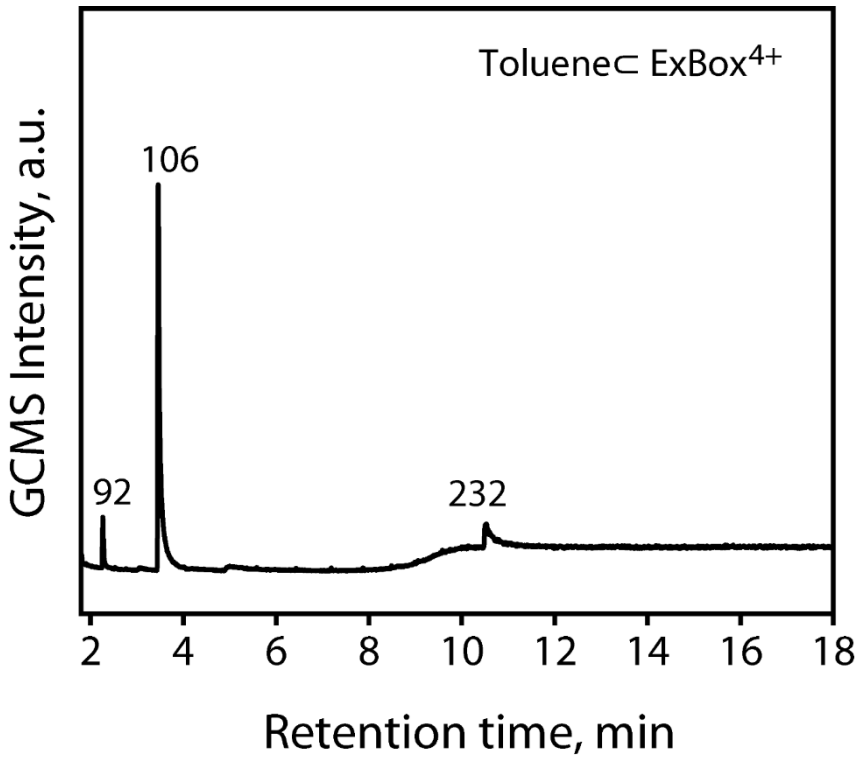

Figure S19. GCMS traces of photoproducts of Toluene⊂ ExBox^{4+} in CH_3CN. m/z= 232 corresponds to ExBipy unit from ExBox^{4+} cavity.

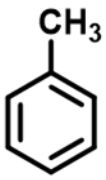

92

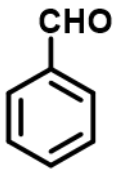

106

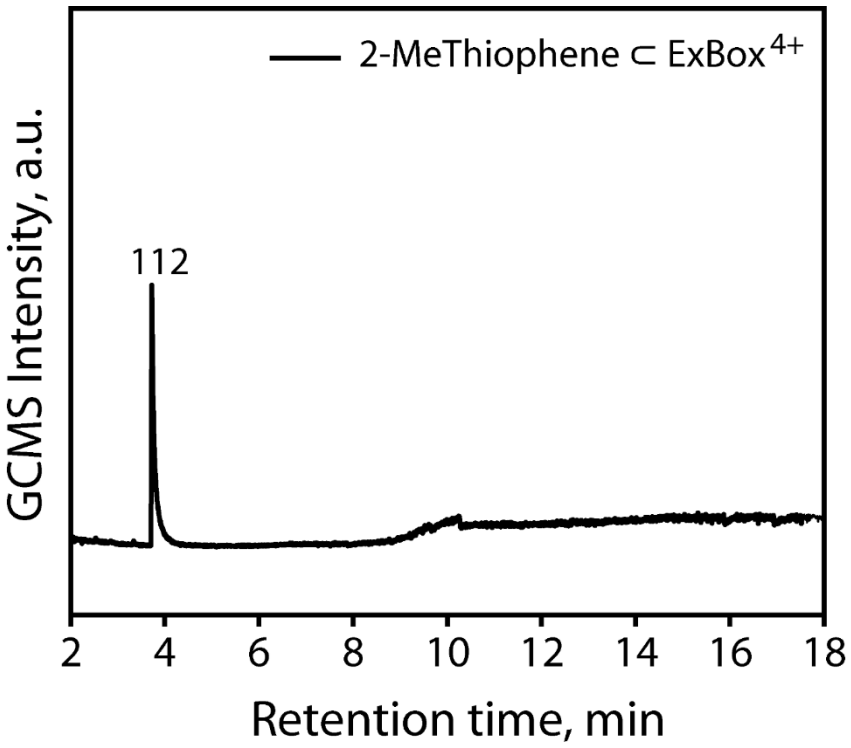

Figure S20. GCMS traces of photoproducts of 2-Methylthiophene⊂ ExBox^{4+} in CH_3CN.

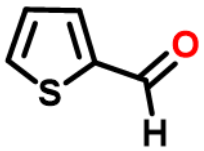

112

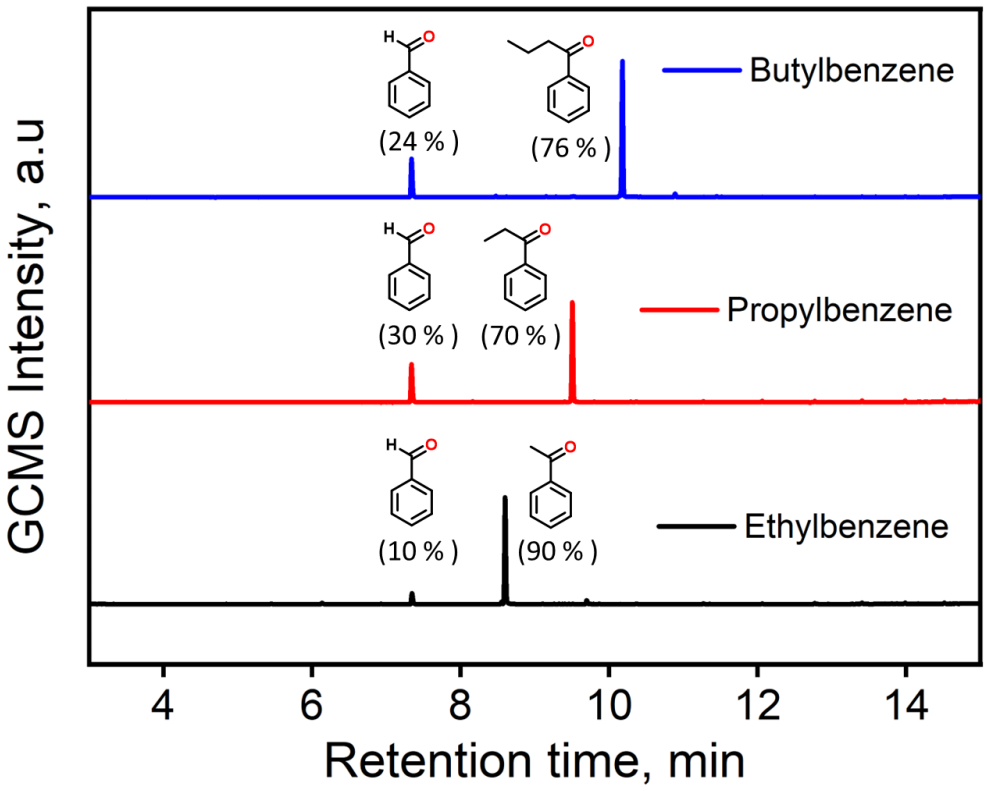

Figure S21. GCMS Traces of Photoproducts of Ethylbenzene, Propylbenzene and Butylbenzene in ExBox with 400 nm LED after 24 hours.

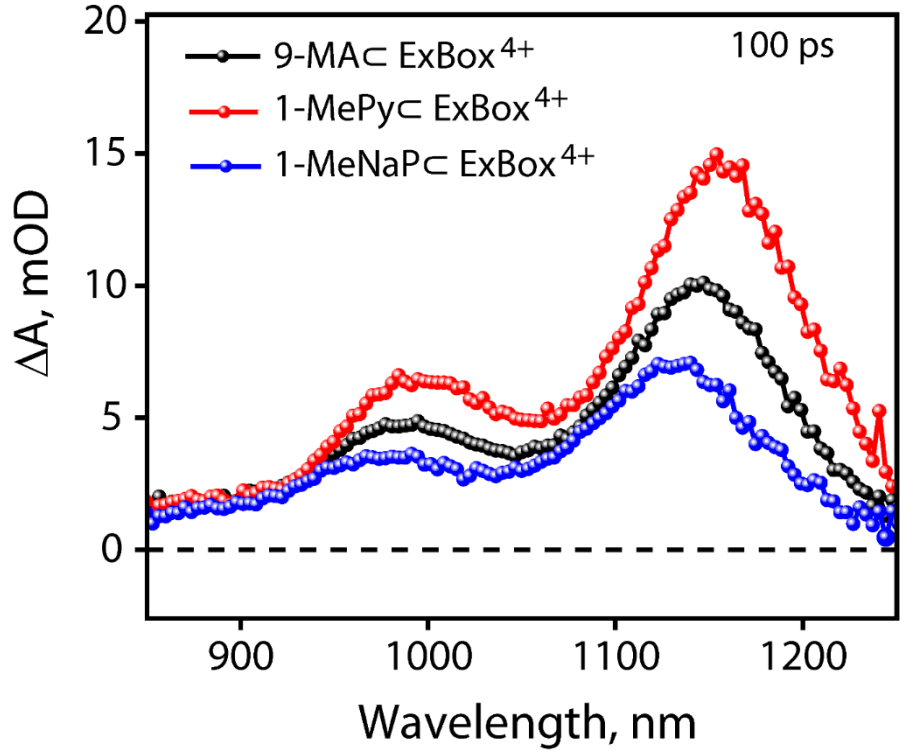

Figure S22. SVD of Transient absorption of 9-MA⊂ ExBox^{4+}, 1-MePy⊂ ExBox^{4+}, 1-MeNap ⊂ ExBox^{4+} in CH_3CN with a 3-state sequential model at 100 ps (NIR region).

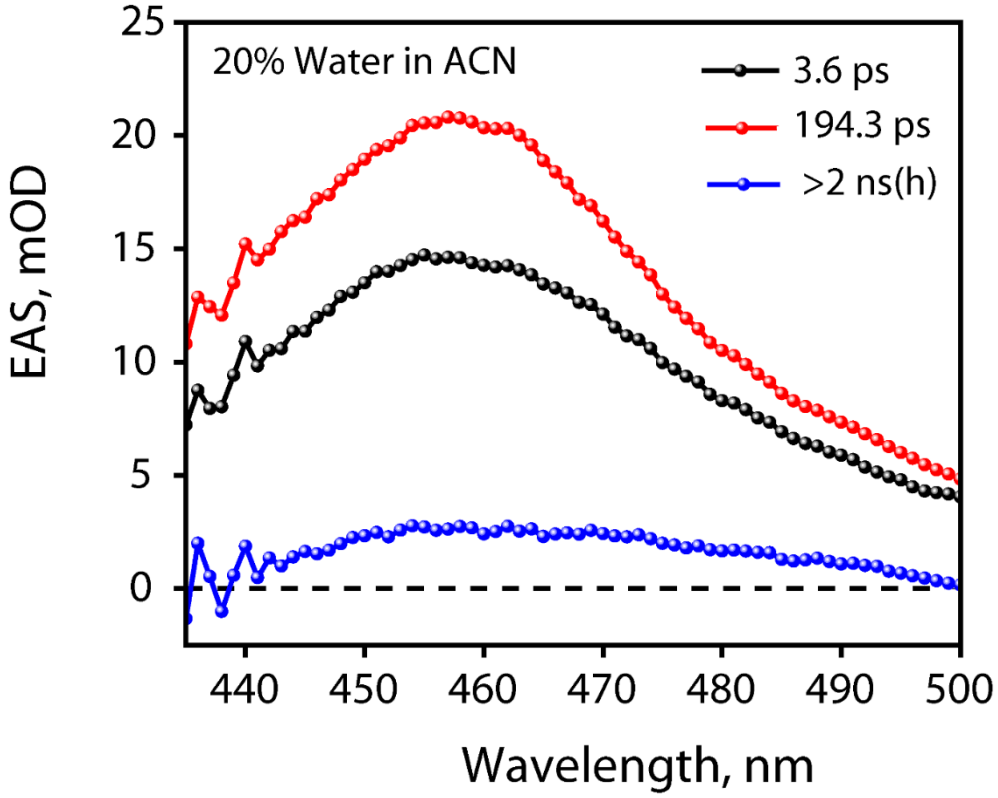

Figure S23. SVD of Transient absorption of 1-MePy ⊂ ExBox^{4+} in 20 % Water +CH_3CN (ACN) with a 3-state sequential model. λ_{exc} = 520 nm[5].

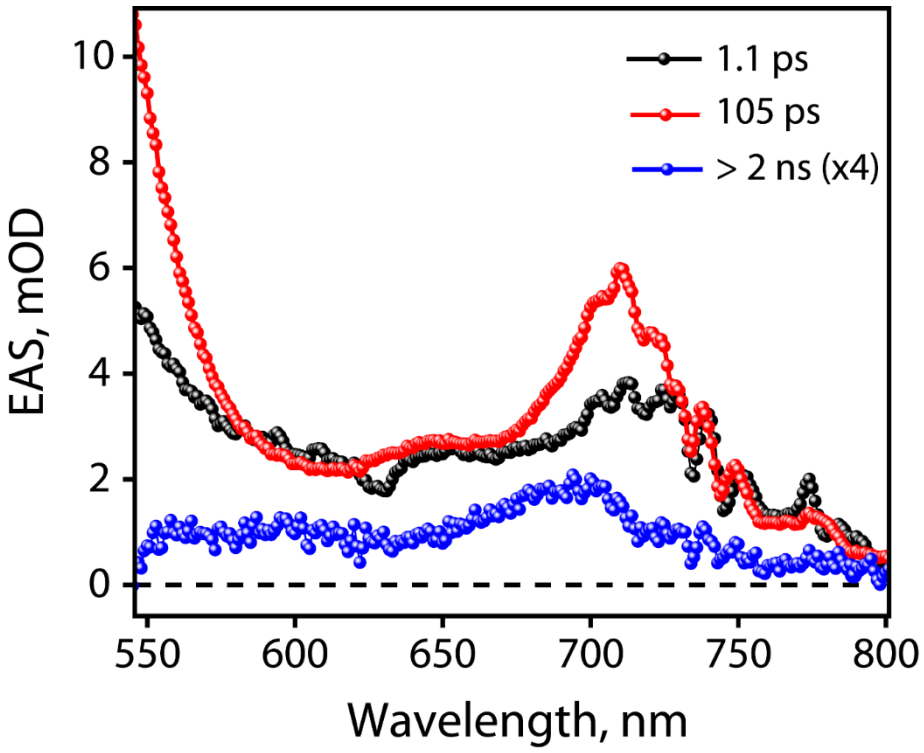

Figure S24. SVD of Transient absorption of 9-MA ⊂ ExBox^{4+} in CH_3CN with a 3-state sequential model[4]. λ_{exc} = 520 nm.

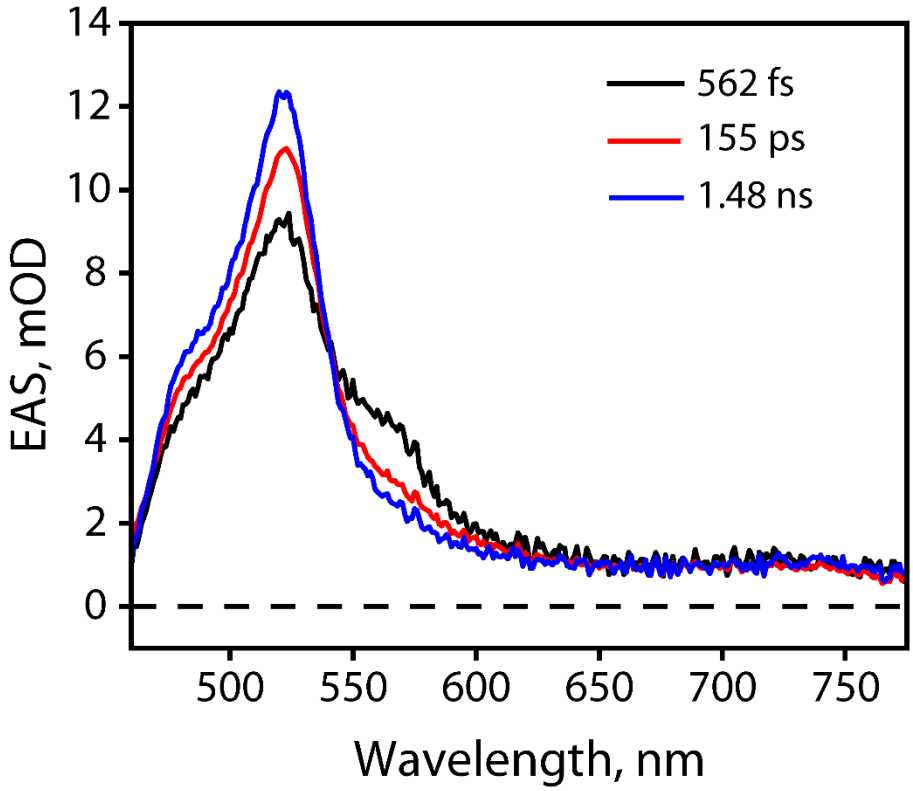

Figure S25. SVD of Transient absorption of 1-MeNap ⊂ ExBox^{4+} in CH_3CN with a 3-state sequential model. λ_{exc} = 400 nm.

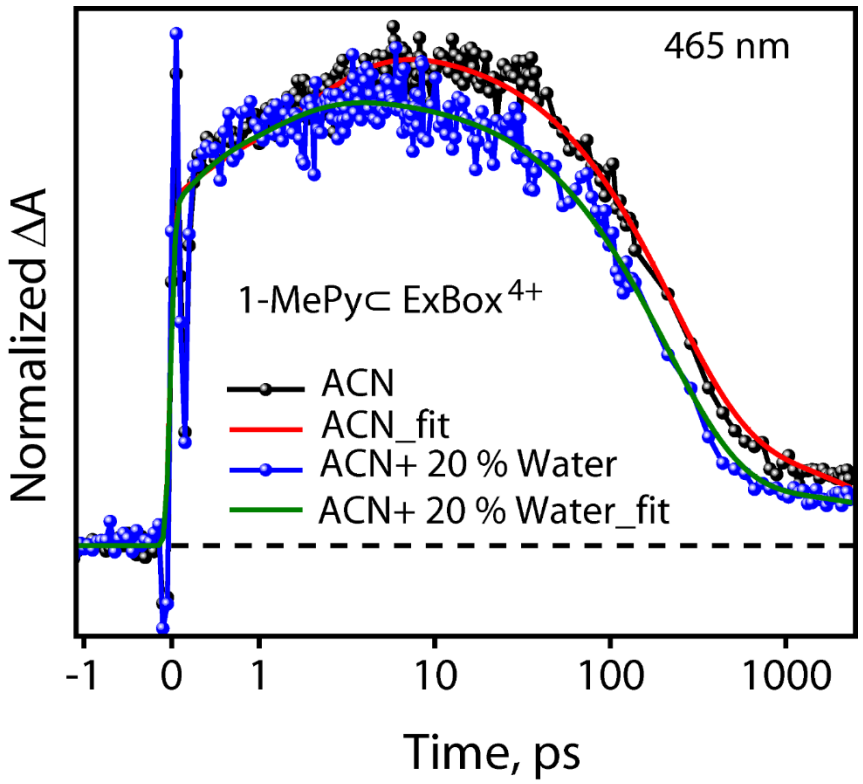

Figure S26. Normalized single wavelength kinetics of Transient absorption of 1-MePy ⊂ $ExBox^{4+}$ in CH_3CN (ACN) and 20 % water+ CH_3CN (ACN) mixture showing faster decay of radical cation after water addition (Blue Dots).

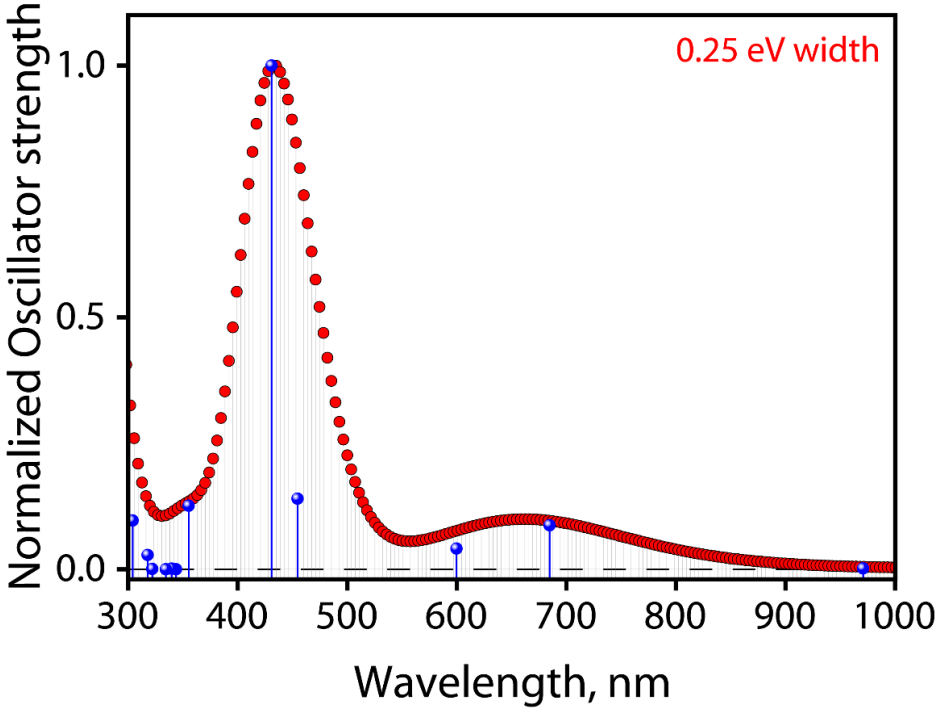

Figure S27. Calculated most-probable transition of 1-MePy radical cation in Acetonitrile dielectric medium from TD-DFT.

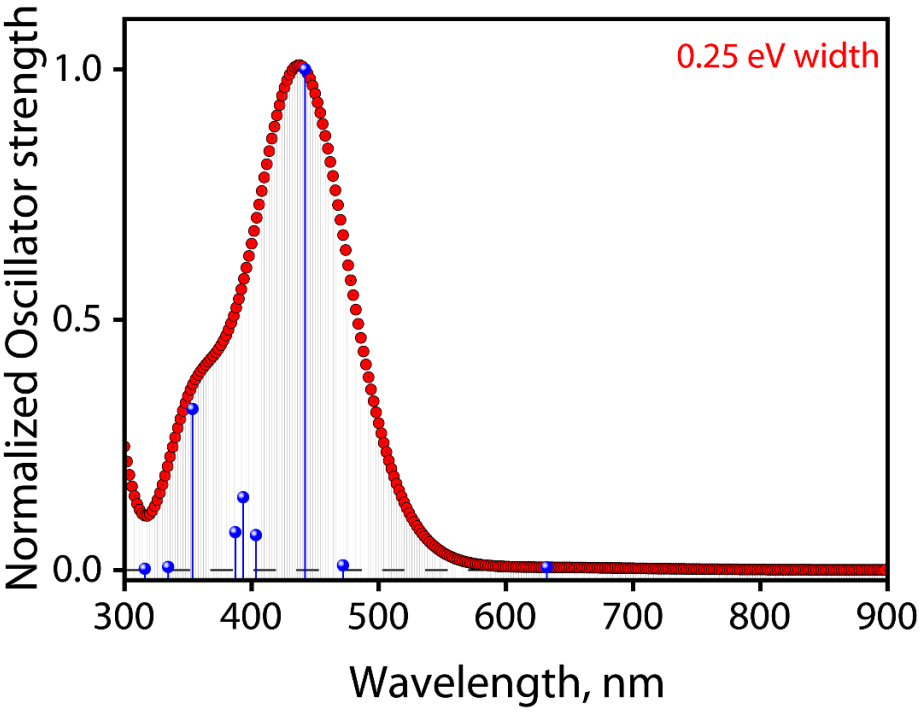

Figure S28. Calculated most-probable transition of 1-MePy neutral radical in Acetonitrile dielectric medium from TD-DFT.

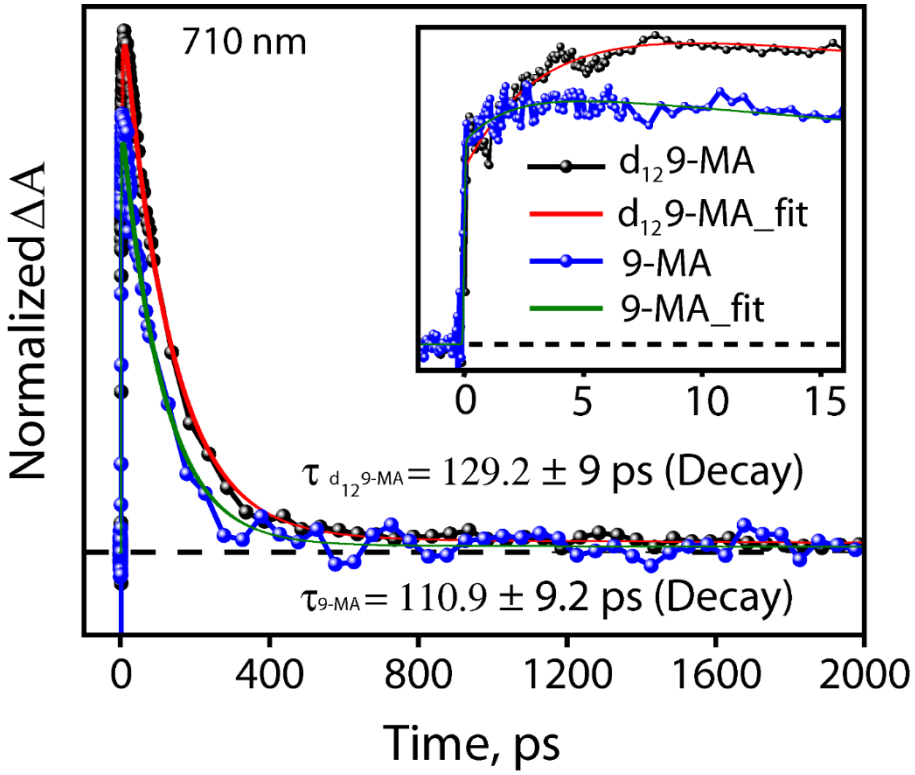

Figure S29. Normalized single wavelength kinetics of Transient absorption of 9-MA ⊂ $ExBox^{4+}$ and d_{12} 9-MA ⊂ $ExBox^{4+}$ in CH_3CN showing slower decay in d_{12} 9-MA as guest.

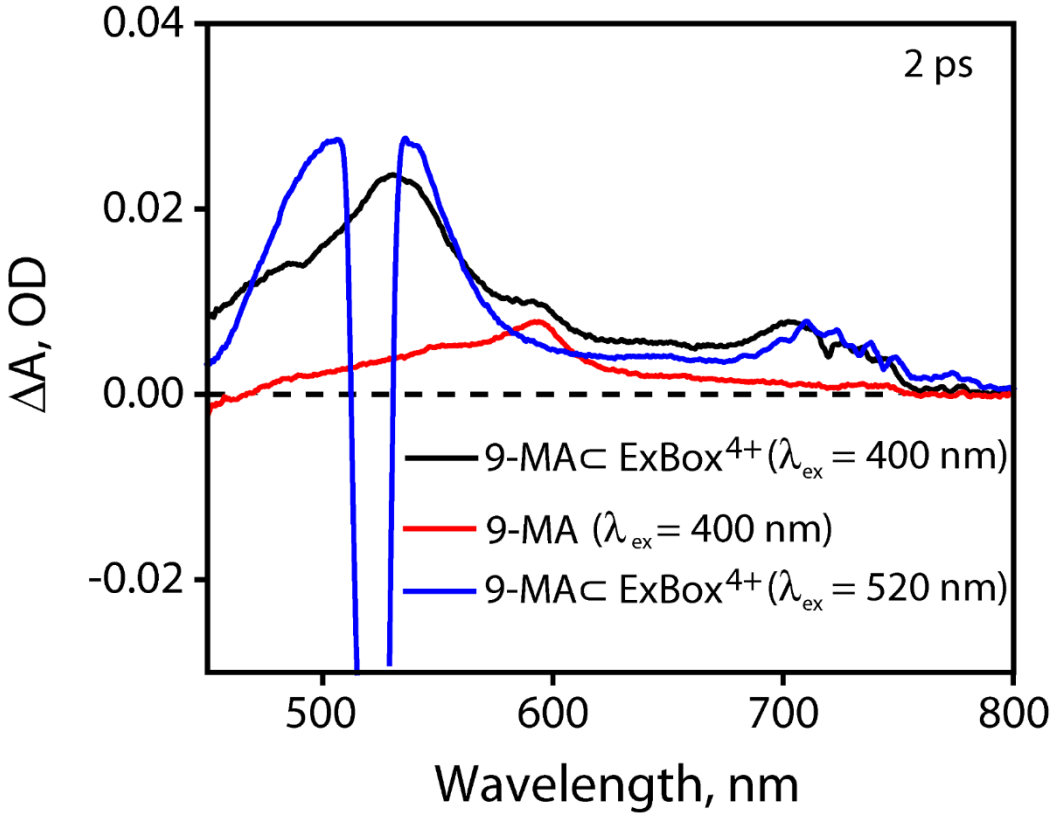

Figure S30. Wavelength dependant Transient absorption spectra showing selective photoexcitation of host-guest complex in CH_3CN with 520 nm excitation[6].

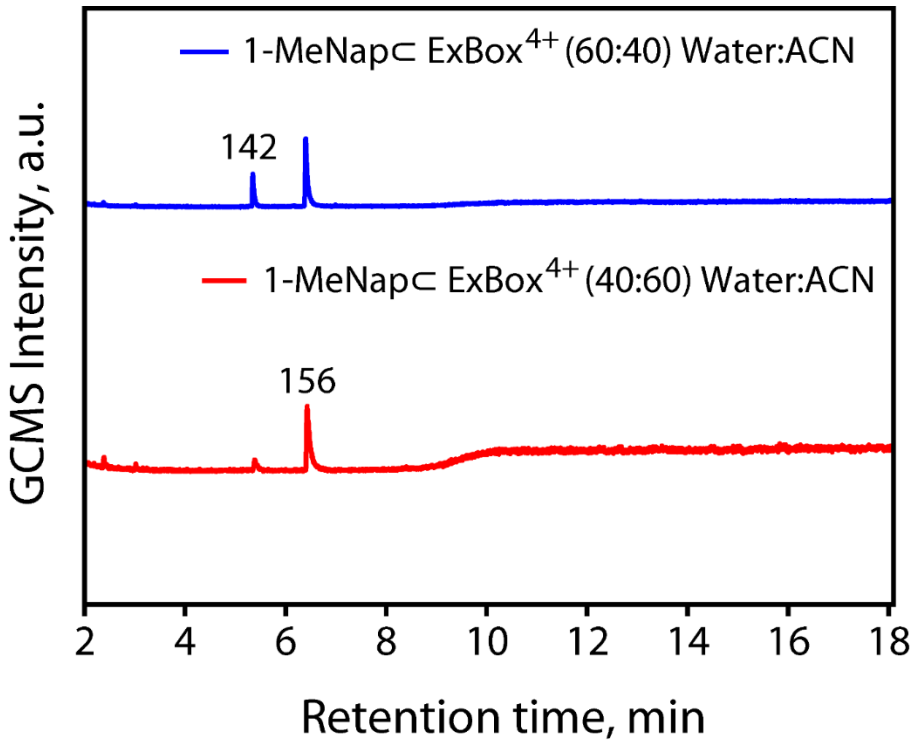

Figure S31. GCMS traces of photoproducts of 1-MeNap⊂ $ExBox^{4+}$ in different Water: CH_3CN (ACN) ratio.

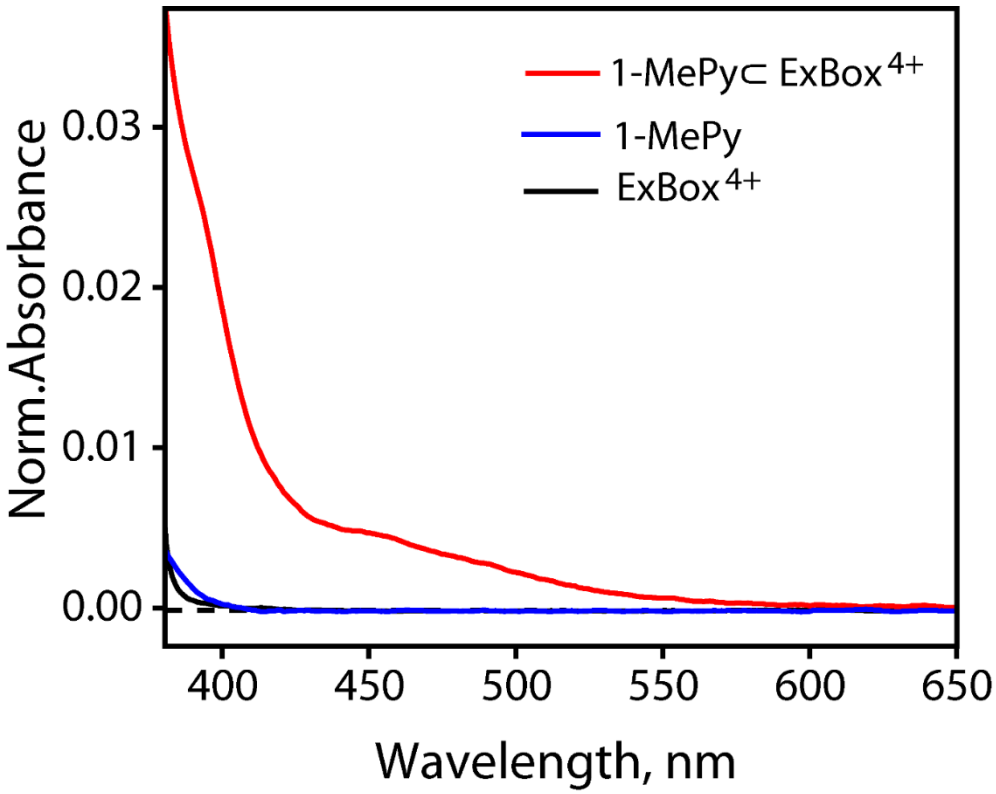

Figure S32. Steady state absorption spectra of $ExBox^{4+}$, 1-MePy and 1-MePy⊂ $ExBox^{4+}$ in ACN. Formation of CT complex shown by red trace in 1-MePy⊂ $ExBox^{4+}$.

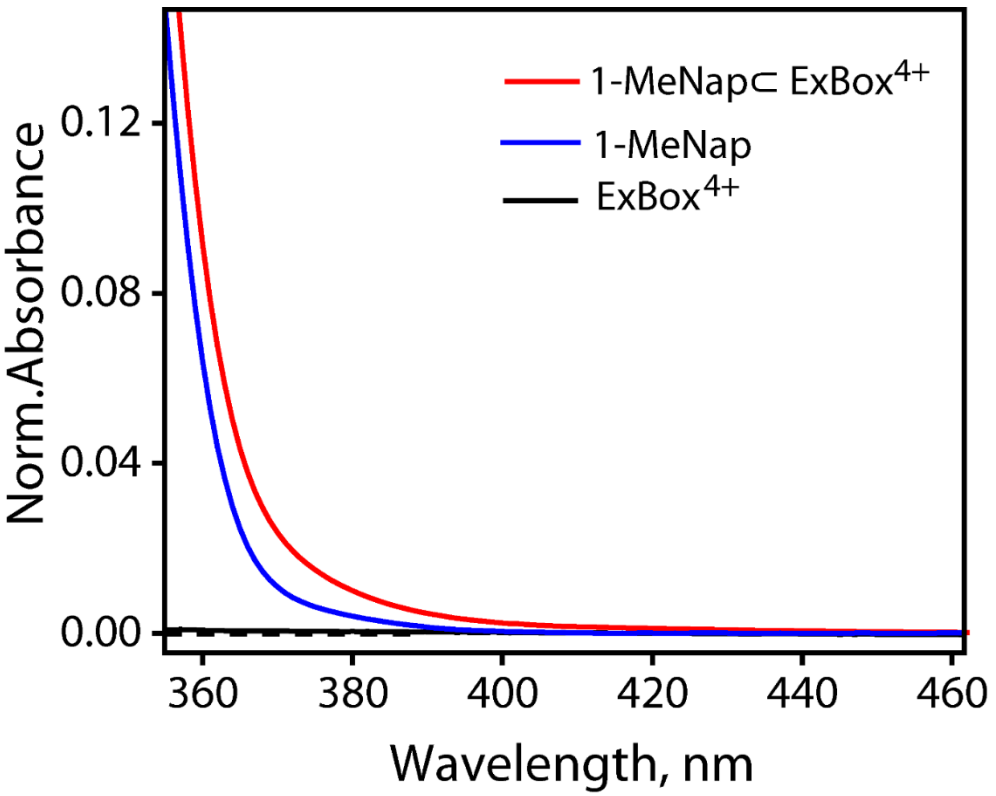

Figure S33. Steady state absorption spectra of $ExBox^{4+}$, 1-MeNap and 1-Menap⊂ $ExBox^{4+}$ in ACN. Formation of CT complex shown by red trace in 1-MeNap⊂ $ExBox^{4+}$.

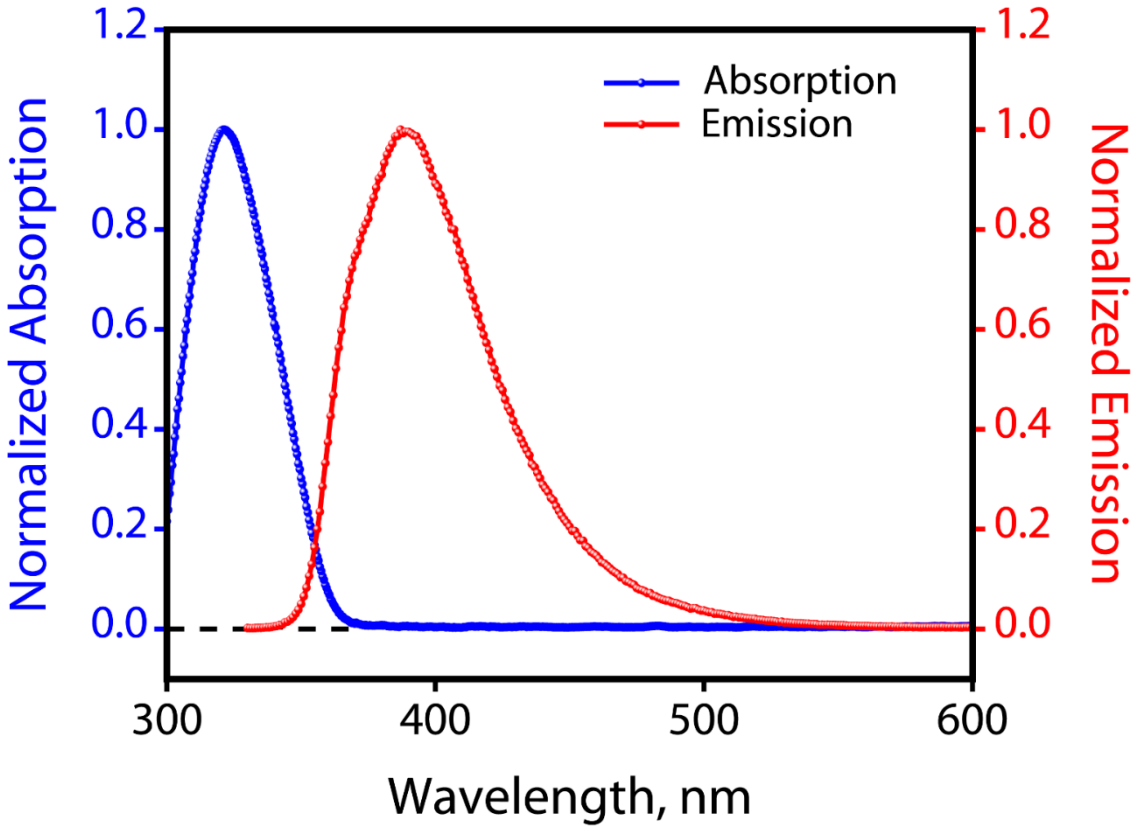

Figure S34. Normalized steady state absorption and emission spectra of $ExBox^{4+}$ in ACN.

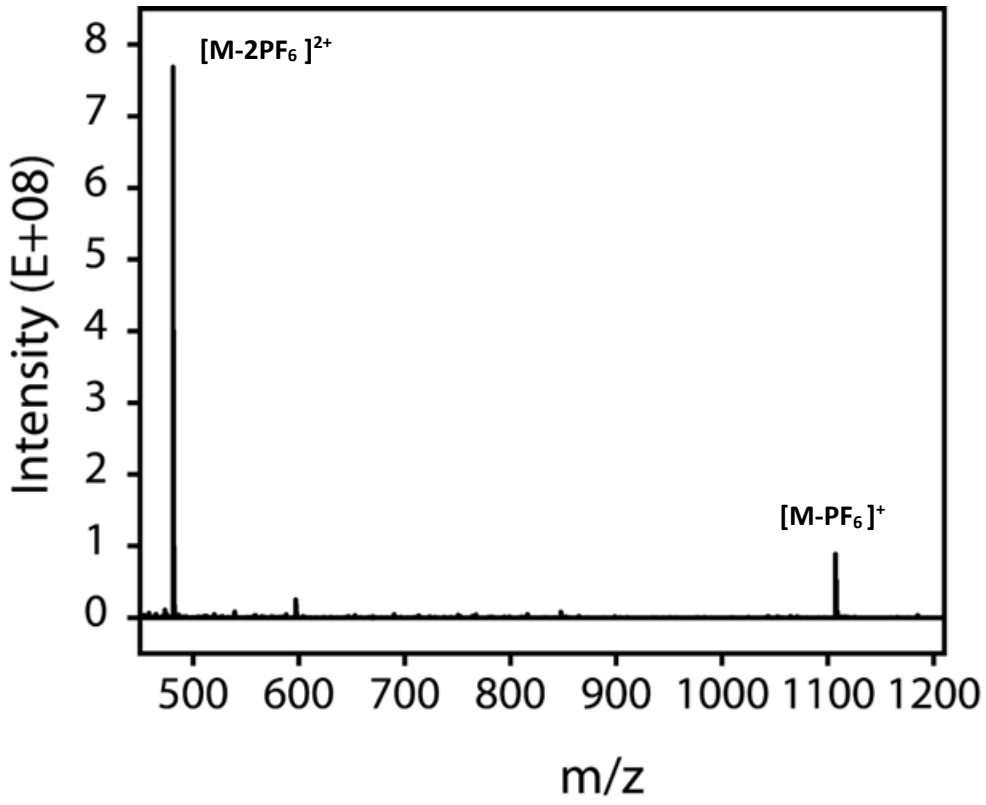

Figure S35. ESI-MS of EXBOX.4PF_6 in ACN. m/z = 1107.218 [M-PF_6]$^+$, m/z = 481.127 [M-2PF_6]$^{2+}$

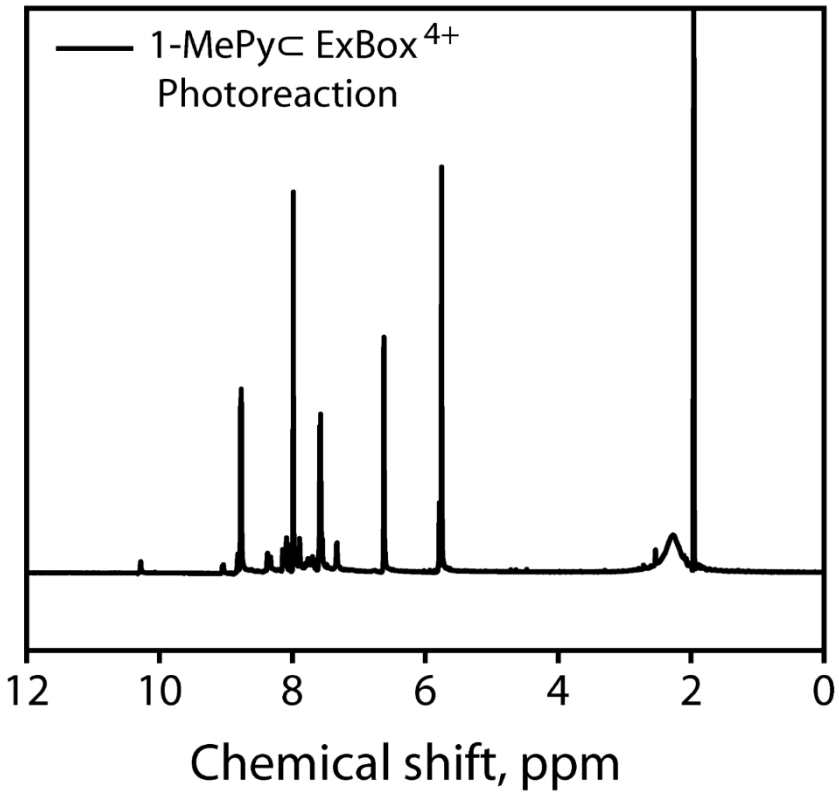

Figure S36. ^{1}H NMR trace of photoreaction of 1-MePy⊂ ExBox^{4+}. Cavity proton peaks are marked with red (a-e), Showing stability of photocatalyst after reaction. S -denotes NMR solvent

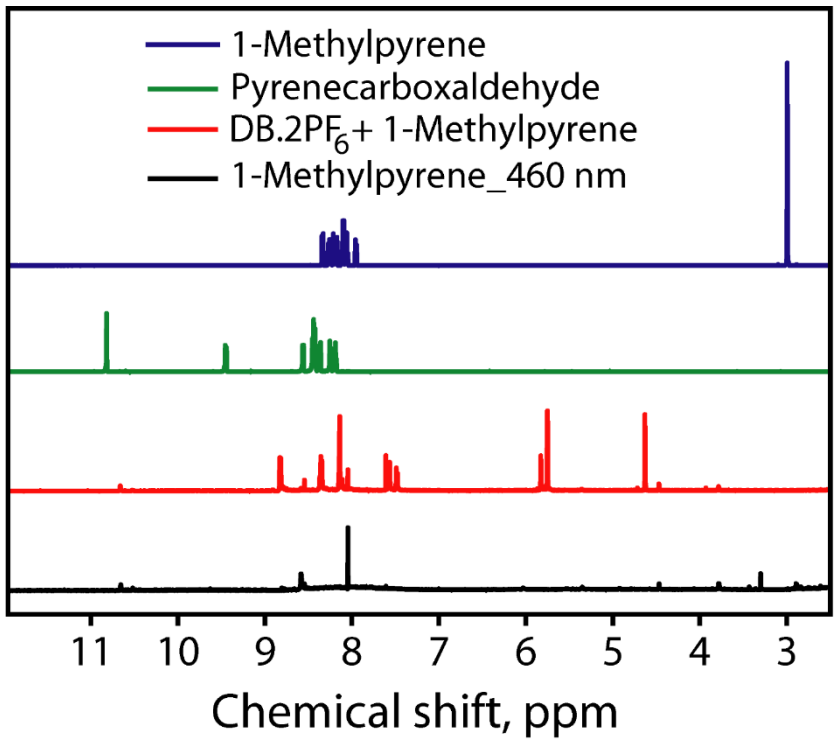

Figure S37. ^{1}H NMR traces of control photoreactions of 1-Methylpyrene at 460 nm LED source. Control reactions shows no aldehyde formation after direct excitation or use of DB.2PF$_6$ as a catalyst.

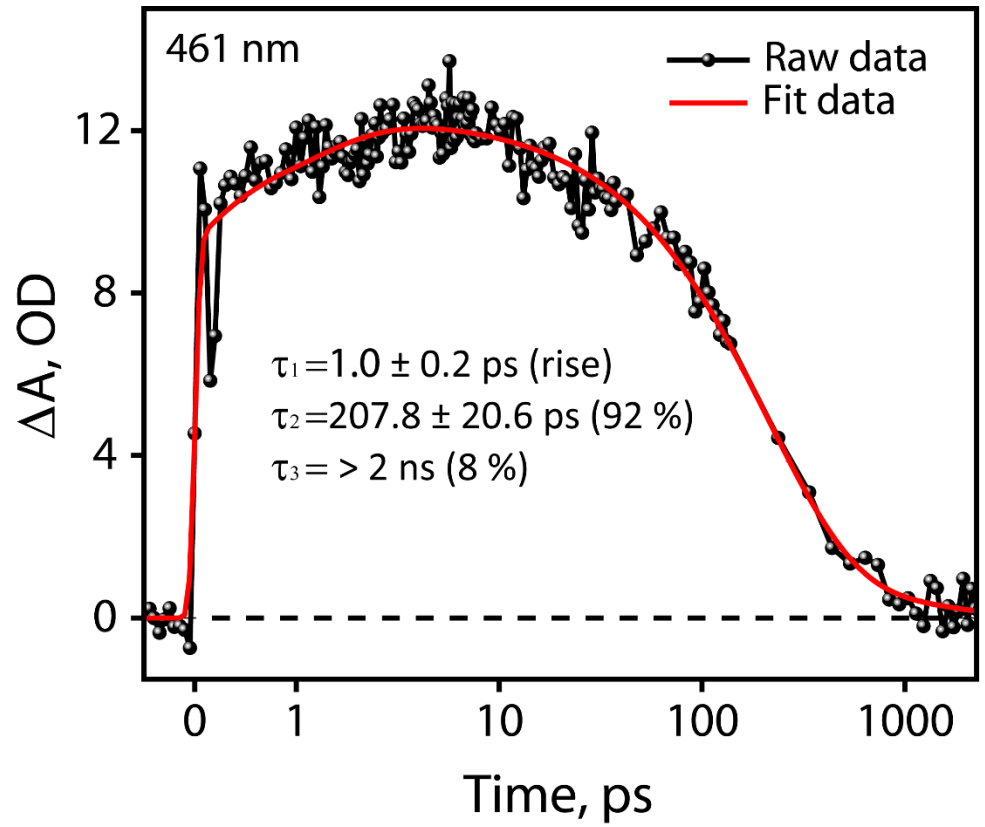

Figure S38. Single wavelength kinetics of Transient absorption of 1-MePy ⊂ ExBox^{4+} in visible region at 461 nm.

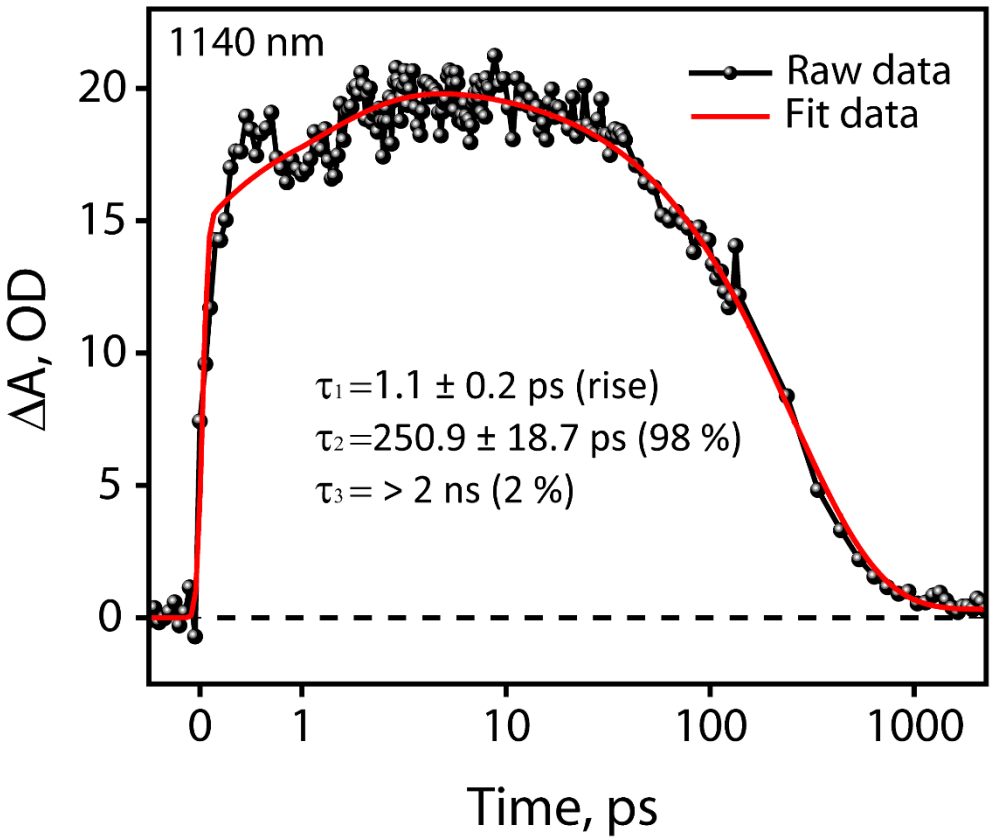

Figure S39. Single wavelength kinetics of Transient absorption of 1-MePy ⊂ ExBox^{4+} in NIR region at 1140 nm.

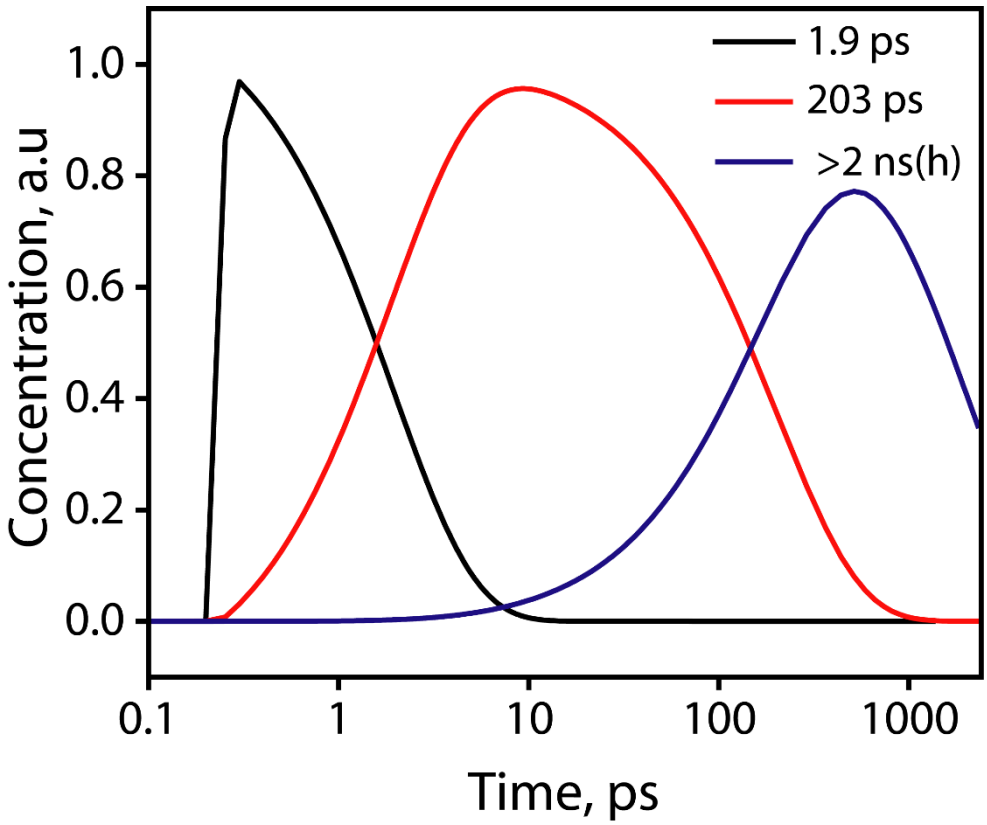

Figure S40. Population analysis of Transient absorption of 1-MePy ⊂ ExBox^{4+} in CH_3CN after SVD analysis with a 3-state sequential model.

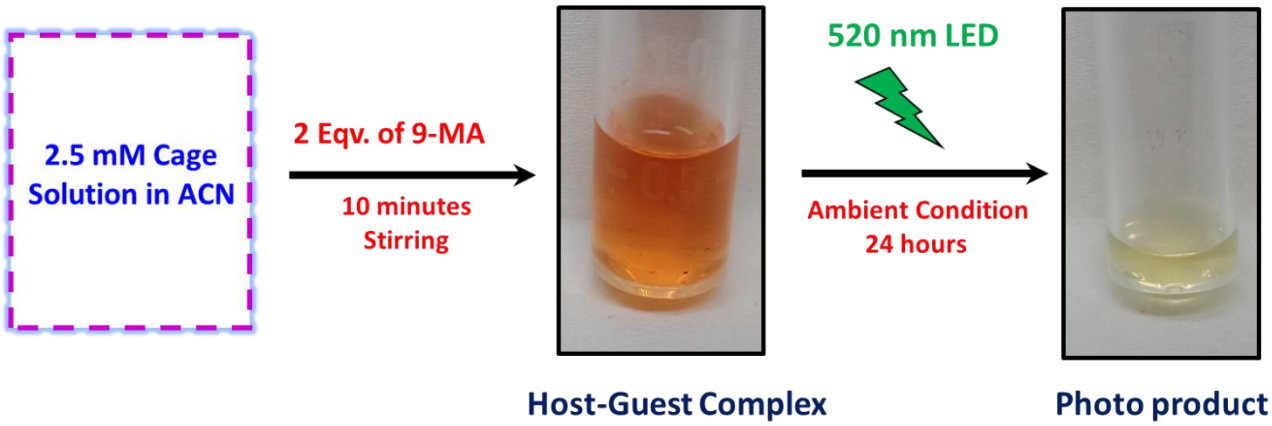

Figure S41.: Visible light triggered photoreaction protocol via Host-guest CT excitation with commercially available LEDs, Light Intensity 50-175 mW/cm^2.

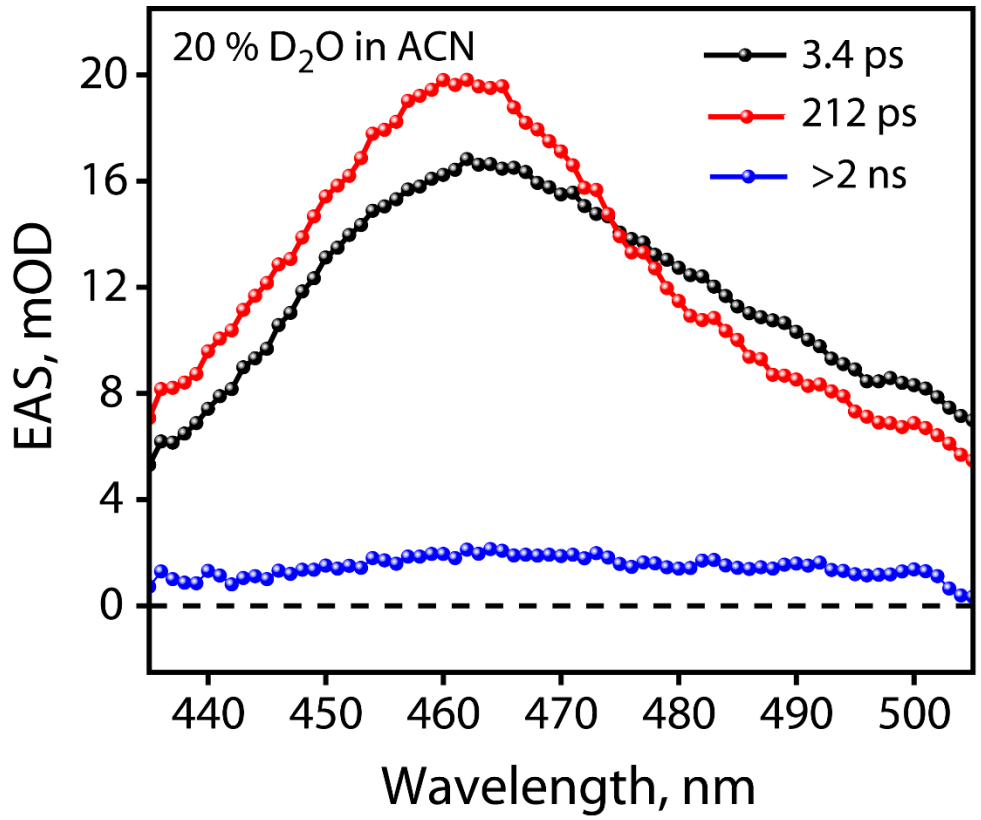

Figure S42. SVD of Transient absorption of 1-MePy ⊂ ExBox^{4+} in 20 % D_2O + CH_3CN (ACN) with a 3-state sequential model. λ_{exc} = 520 nm.

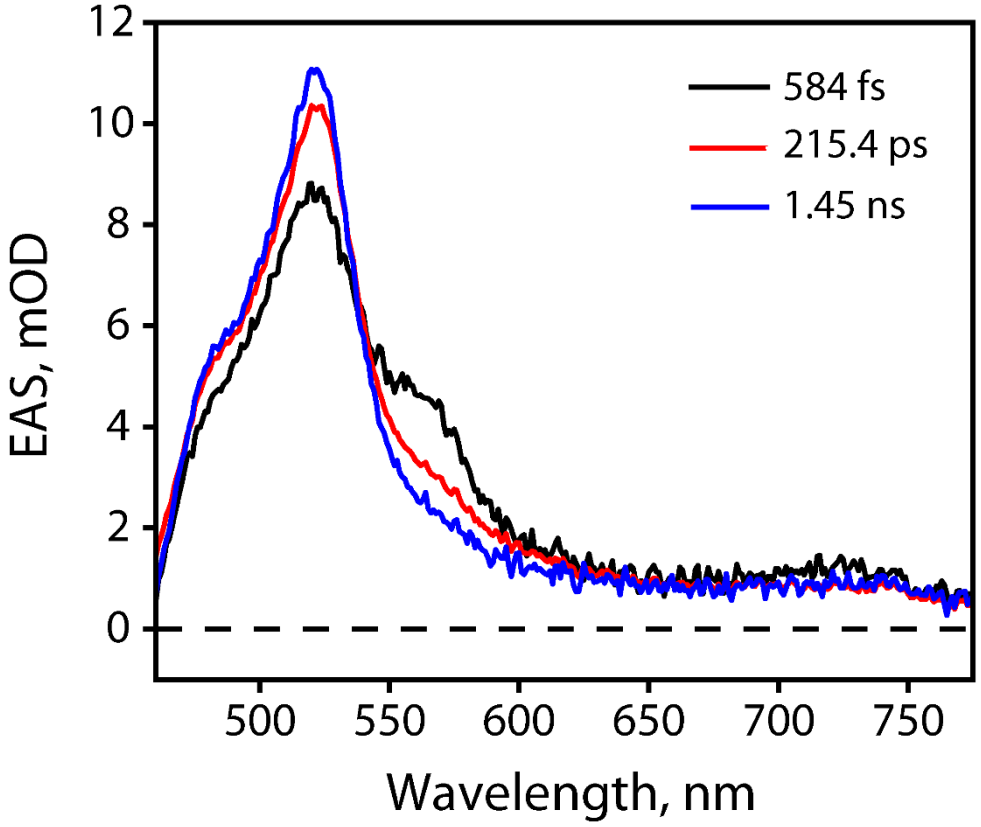

Figure S43. SVD of Transient absorption of 1-MeNap ⊂ ExBox^{4+} in CD_3CN with a 3-state sequential model. λ_{exc} = 400 nm.

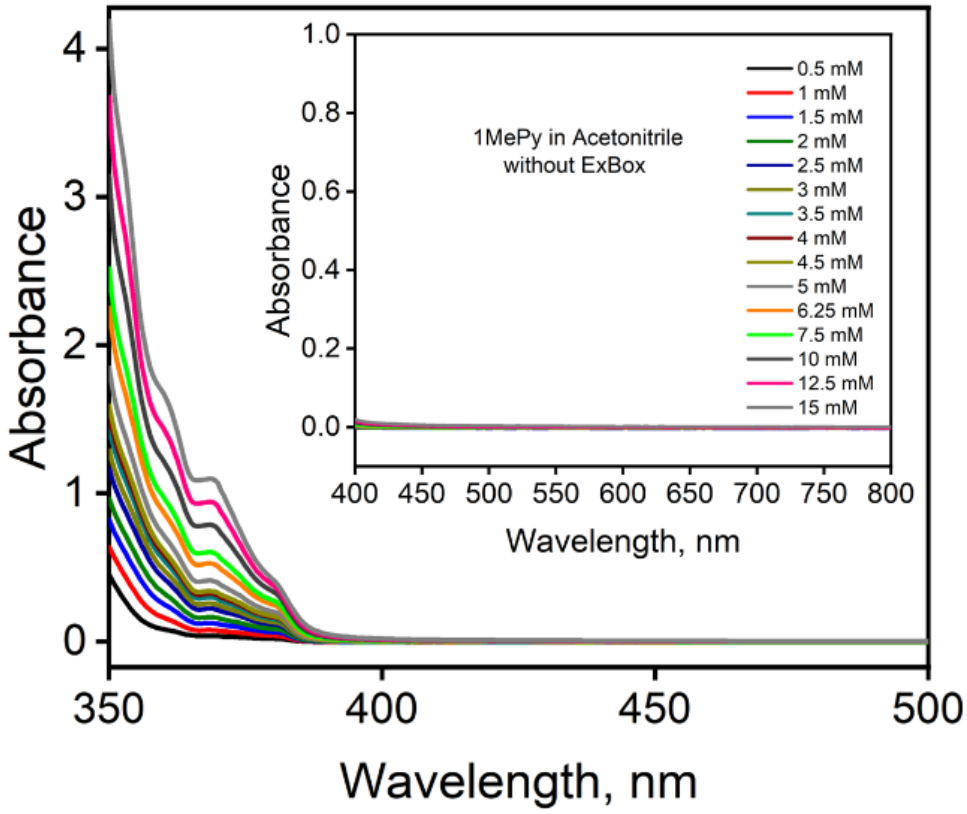

Figure S44. UV-Vis titration of 1MePy in Acetonitrile without ExBox addition.

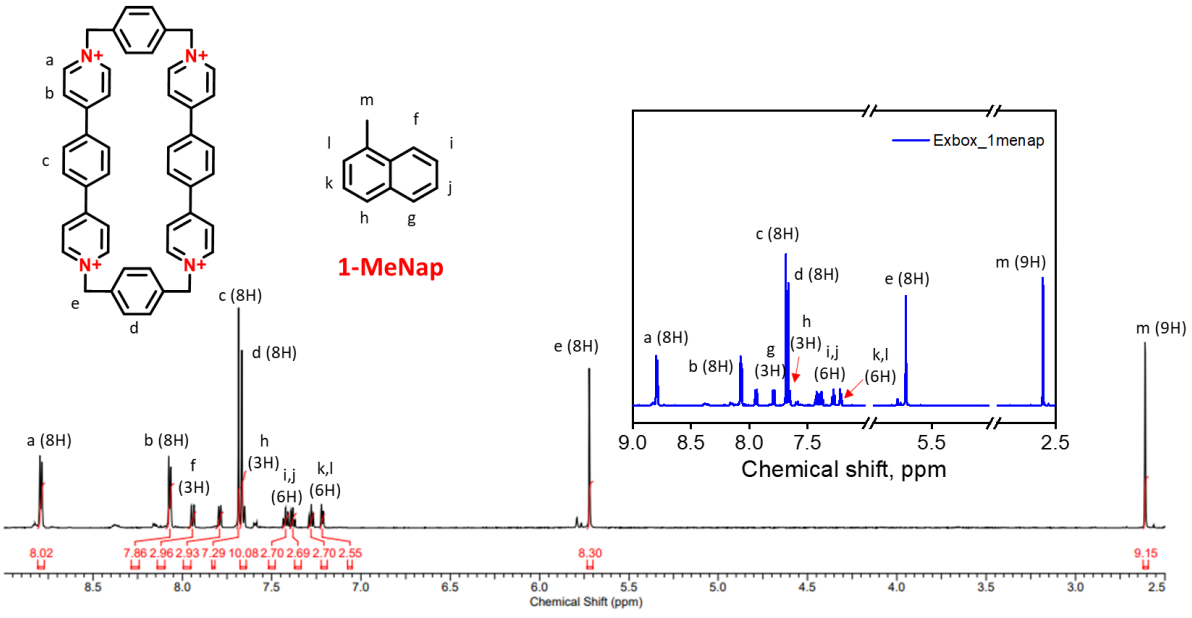

Figure S45. ^{1}H NMR spectra of 1-MeNap ⊂ ExBox host-guest complex in CD3CN, 600 MHz showing peak area integrations.

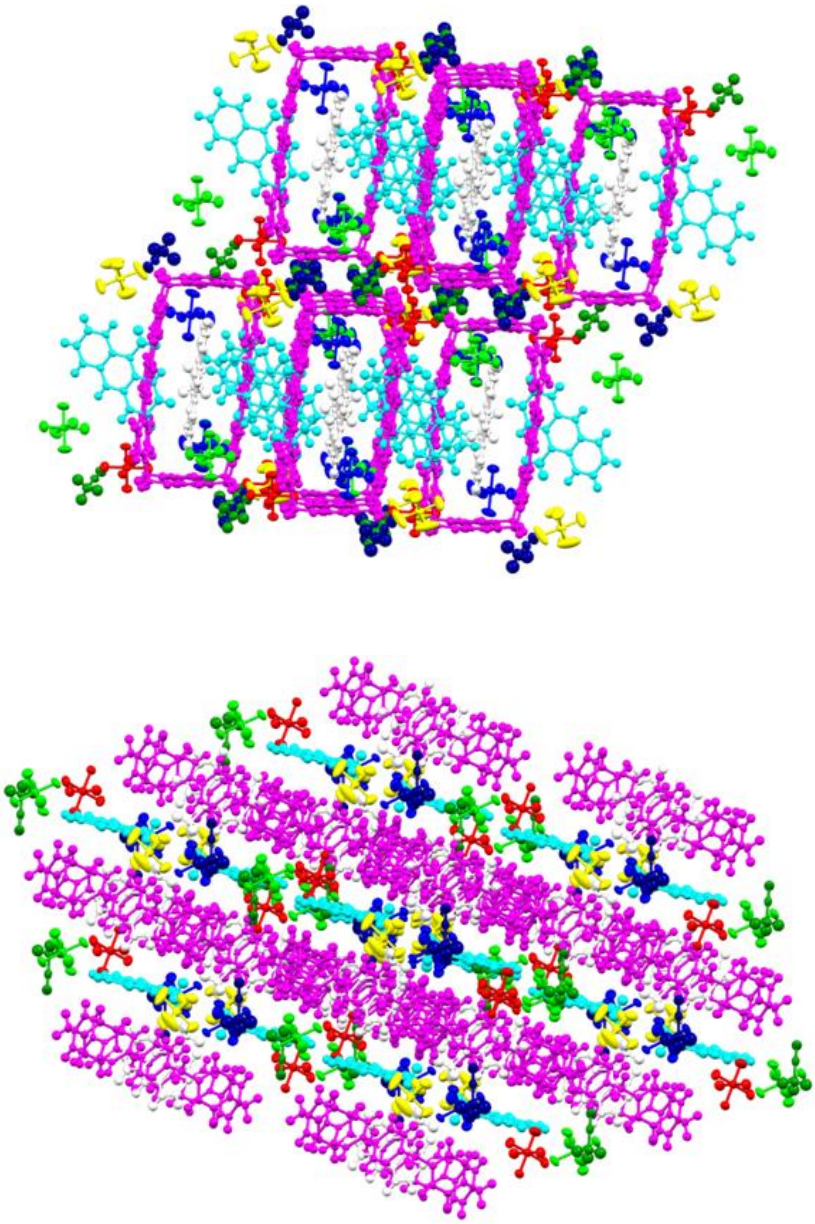

Crystal Parameters. $[C_{48}H_{40}N_4 \subset C_{15}H_{12}.(PF_6)_4].(C_{15}H_{12}).(CH_3CN)_2$; Orange (0.24 × 0.12 × 0.02 mm); Monoclinic, P-1(2), a = 12.374(5), b = 16.879(5), c = 19.484(8) Å, α = 66.889(3), β = 79.115(3), γ = 85.113 (3)°, V = 3675.6(3) $Å^3$, Z = 2, T = 150(10) K, ρ_{calc} = 1.553 g cm^{-3} , μ = 0.217 mm^{-1} . Of a total of 159688 reflections which were collected, 12931 were unique (R_{int} = 0.1403). Final $R_1(F^2 > 2\sigma F^2)$ = 0.0622 and wR_2 = 0.1917.

Figure S46. Single crystal structure of 9-MA ⊂ExBox.4PF_6 host guest complex. Pink colour denotes $ExBox^{4+}$ unit, cyan and white corresponds to 9-MA molecules, rest are counter anions (PF_6^-) and solvent molecules (CH_3CN).

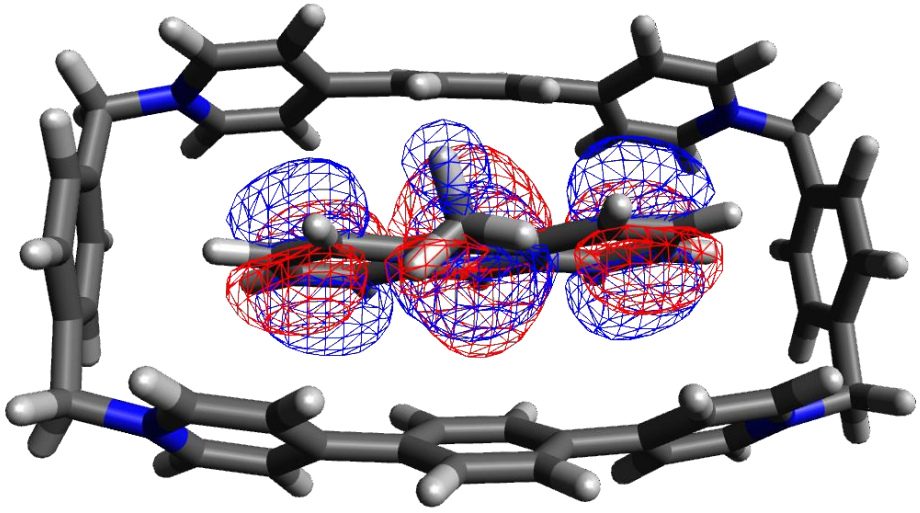

HOMO

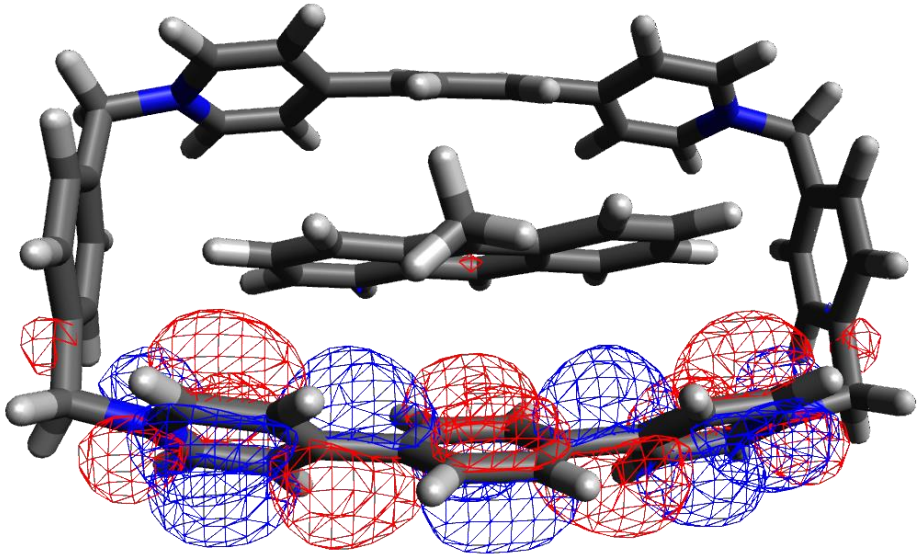

LUMO

Figure S47. HOMO-LUMO electron densities of 9-MA ⊂ExBox (1:1) host guest complex. Initial coordinates taken from crystal structure. wb97xd/6-311G(d,p) basis set used for calculation .

Supporting Table 1:

1-MePy radical cation optimized geometry coordinates in Acetonitrile

C	2.78267700	-0.37454500	-0.00000200
C	1.38752600	-0.74024200	-0.00000300
C	0.39068500	0.28666900	-0.00000200
C	0.77239700	1.66344200	-0.00000100
C	2.16009300	1.98608400	0.00000100
C	3.12805300	0.98856600	0.00000100
C	0.96386900	-2.09607300	-0.00000300
C	-0.38282300	-2.43135600	-0.00000100
C	-1.38624600	-1.42773500	-0.00000100
C	-0.98901100	-0.05633400	-0.00000200
C	-1.98409300	0.97051400	0.00000000
C	-1.57580200	2.33101300	-0.00000100
C	-0.22951300	2.66803300	-0.00000100
C	-2.77476000	-1.74795600	0.00000100
C	-3.74284600	-0.74254100	0.00000300
C	-3.35907900	0.60061600	0.00000200
C	3.86324100	-1.41891600	0.00000400
H	2.45758100	3.02931700	0.00000200
H	4.17628600	1.26311500	0.00000200
H	1.70140500	-2.88844400	-0.00000300
H	-0.67806200	-3.47492500	-0.00000100
H	-2.33056100	3.10954500	-0.00000100
H	0.06855500	3.71074100	-0.00000100
H	-3.07318300	-2.79087800	0.00000100
H	-4.79388500	-1.00395900	0.00000500
H	-4.11217500	1.38151600	0.00000400
H	4.85145400	-0.95537400	-0.00005000
H	3.79321600	-2.06800100	0.88163700
H	3.79315600	-2.06808600	-0.88156100

Supporting Table 2:

1-MePy neutral radical optimized geometry coordinates in Acetonitrile

C	2.82571900	-0.50093600	-0.00001200
C	1.40059800	-0.81750400	-0.00000300
C	0.44144800	0.24521000	0.00001300
C	0.86627900	1.61699800	0.00001300
C	2.26204600	1.90160500	-0.00001400
C	3.19451600	0.89382100	-0.00002600
C	0.91715700	-2.16103900	-0.00001500
C	-0.42672700	-2.44959300	-0.00000100
C	-1.41037200	-1.40957200	0.00001700
C	-0.96104800	-0.05019900	0.00001800
C	-1.92537600	1.01301000	0.00000800
C	-1.45774600	2.36944900	0.00000500
C	-0.11304800	2.65385100	0.00000700
C	-2.79786000	-1.68057400	-0.00000200
C	-3.72684400	-0.63841600	-0.00001400
C	-3.30010800	0.69358100	-0.00000800
C	3.82949300	-1.46329200	0.00003700
H	2.58169000	2.93956200	-0.00001300
H	4.25302500	1.13560700	-0.00006300
H	1.62566900	-2.98070500	-0.00004100
H	-0.76194200	-3.48244900	0.00000900
H	-2.18987300	3.17112300	0.00000500
H	0.22714200	3.68529800	0.00001100
H	-3.13398600	-2.71298200	-0.00001400
H	-4.78852800	-0.86280900	-0.00003100
H	-4.02840800	1.49897700	-0.00000900
H	4.87154800	-1.16196700	0.00003500
H	3.63489400	-2.52805600	-0.00002700

Supporting Table 3:

The TD-DFT oscillator strengths and the excitation energies computed using the optimized geometry of 1-MePy radical cation in Acetonitrile.

	Excitation energies	Oscillator Strengths:
Excited State 1:	1.2772 eV 970.78 nm	f= 0.0005
Excited State 2:	1.8106 eV 684.75 nm	f=0.0304
Excited State 3:	2.0672 eV 599.76 nm	f= 0.0143
Excited State 4:	2.7274 eV 454.59 nm	f= 0.0489
Excited State 5:	2.8770 eV 430.95 nm	f= 0.3488
Excited State 6:	3.4892 eV 355.34 nm	f= 0.0440
Excited State 7:	3.6068 eV 343.75 nm	f= 0.0000
Excited State 8:	3.6502 eV 339.67 nm	f= 0.0004
Excited State 9:	3.7067 eV 334.48 nm	f= 0.0000
Excited State 10:	3.8508 eV 321.97 nm	f= 0.0002

Supporting Table 4:

The TD-DFT oscillator strengths and the excitation energies computed using the optimized geometry of 1-MePy neutral radical in Acetonitrile.

	Excitation energies	Oscillator Strengths:
Excited State 1:	1.9610 eV 632.24 nm	f= 0.0020
Excited State 2:	2.6275 eV 471.88 nm	f=0.0034
Excited State 3:	2.8047 eV 442.05 nm	f= 0.3693
Excited State 4:	3.0734 eV 403.41 nm	f= 0.0257
Excited State 5:	3.1520 eV 393.35 nm	f= 0.0536
Excited State 6:	3.2021 eV 387.19 nm	f= 0.0279
Excited State 7:	3.5066 eV 353.57 nm	f= 0.1188
Excited State 8:	3.7071 eV 334.45 nm	f= 0.0022
Excited State 9:	3.9231 eV 316.03 nm	f= 0.0009

Excited State 10: 4.1849 eV 296.26 nm f= 0.0043

Supporting Table 5:

9-MA in ExBox optimized geometry coordinates

N	-5.54839500	3.35187000	0.08789100
N	-5.68157400	-3.23646700	-0.07103100
N	5.70531600	3.28703500	-0.00486800
N	5.57297200	-3.30233800	-0.19494200
C	-7.14393200	1.48400400	0.04035500
C	-7.21455900	0.75836400	1.22750600
H	-7.26835100	1.27036300	2.18243200
C	-7.24458900	-0.63002100	1.20042500
H	-7.32056200	-1.17587300	2.13496600
C	-7.20496300	-1.31124200	-0.01411100
C	-7.20185500	-0.58374000	-1.20294100
H	-7.24364600	-1.09404100	-2.15941600
C	-7.17101700	0.80384100	-1.17558700
H	-7.19069100	1.35274100	-2.11139000
C	-6.99735900	2.98833300	0.07066200
H	-7.44323300	3.46136400	-0.80380200
H	-7.45520100	3.42747700	0.95670100
C	-4.88436800	3.53080400	-1.06929300
H	-5.47601500	3.51201900	-1.97497500
C	-3.52076100	3.70385200	-1.08640700
H	-3.02925600	3.81002400	-2.04401800
C	-2.79343500	3.69322100	0.10829100
C	-3.52378000	3.57151100	1.29706200
H	-3.03925300	3.62856000	2.26254700
C	-4.88551500	3.39643000	1.25935500
H	-5.48011900	3.28984000	2.15681300
C	-7.11659700	-2.82015900	-0.04069500
H	-7.57115000	-3.27368000	0.83969000

H	-7.59804700	-3.24522700	-0.92098100
C	-4.99662000	-3.36970000	1.08063200
H	-5.56655600	-3.28157000	1.99605000
C	-3.63893500	-3.58270300	1.07791900
H	-3.13069500	-3.65898800	2.03013200
C	-2.93786500	-3.65728100	-0.13117600
C	-3.69244200	-3.59003600	-1.30848300
H	-3.23241500	-3.71366800	-2.27959300
C	-5.04769300	-3.37252800	-1.25130100
H	-5.65953000	-3.30222000	-2.14083700
C	-1.31679000	3.76950800	0.11770300
C	-0.61695300	4.50820400	-0.84038000
H	-1.14832100	5.11409400	-1.56512500
C	0.76919900	4.51132100	-0.85164600
H	1.28746300	5.11754300	-1.58578700
C	1.48589700	3.77758700	0.09714400
C	0.78556900	3.06441300	1.07214000
H	1.31909200	2.46370600	1.79879300
C	-0.59695500	3.05943700	1.08087500
H	-1.11464500	2.45632200	1.81632700
C	-1.46281000	-3.74746600	-0.16747300
C	-0.74114700	-4.41913200	0.82309200
H	-1.25424900	-4.97920100	1.59641500
C	0.64498400	-4.41663200	0.80590200
H	1.17746700	-4.97598300	1.56622900
C	1.34183300	-3.74158400	-0.20055900
C	0.61708300	-3.09749700	-1.20533500
H	1.12765100	-2.54193800	-1.98169700
C	-0.76496400	-3.10008000	-1.18905000
H	-1.29826600	-2.54458000	-1.95073300
C	2.96140500	3.69374600	0.06179300

C	3.66187600	3.64626100	-1.14858300
H	3.15110000	3.73466500	-2.09836300
C	5.02050200	3.43853200	-1.15445900
H	5.59128500	3.36849300	-2.07097500
C	5.07069400	3.39719300	1.17784400
H	5.68303800	3.31291900	2.06577800
C	3.71402300	3.60534000	1.23867600
H	3.25036800	3.70566300	2.21090700
C	2.81854300	-3.65854700	-0.19865200
C	3.54979000	-3.63016200	0.99360600
H	3.06248900	-3.71084700	1.95561900
C	4.91223600	-3.45241300	0.96815800
H	5.50575200	-3.40711600	1.87152200
C	4.90744400	-3.38344900	-1.36275500
H	5.49883500	-3.29853600	-2.26470100
C	3.54650500	-3.56832800	-1.39184100
H	3.06214000	-3.65635600	-2.35499600
C	7.14127900	2.87450600	-0.04226400
H	7.62440900	3.29397300	0.83983400
H	7.59251200	3.33501800	-0.92064800
C	7.23085300	1.36586100	-0.07967300
C	7.27667200	0.69175400	-1.29791900
H	7.35733100	1.24300800	-2.22888400
C	7.24326100	-0.69672000	-1.33340100
H	7.29934900	-1.20336100	-2.29102800
C	7.16476300	-1.42903500	-0.15097900
C	7.18669000	-0.75572100	1.06894700
H	7.20248900	-1.30976100	2.00180500
C	7.21939400	0.63123200	1.10477100
H	7.25801100	1.13572400	2.06446800
C	7.02058000	-2.93352800	-0.18813500

H	7.47248700	-3.36686500	-1.07994600
H	7.47513400	-3.40977500	0.68023600
C	1.04589500	-0.26606500	0.86938200
C	2.15507000	-0.41180200	1.76738600
H	1.97625500	-0.63606400	2.81060600
C	3.43848000	-0.23648500	1.34757400
H	4.25533700	-0.33315300	2.05447600
C	3.72513900	0.06778400	-0.01147000
H	4.75464400	0.17606900	-0.33187700
C	2.70599900	0.23644300	-0.89499700
H	2.90864900	0.48281400	-1.93261800
C	1.34170500	0.10796900	-0.48497400
C	0.30562100	0.33671500	-1.38363600
H	0.53514600	0.60680100	-2.40998000
C	-1.02333000	0.22021700	-0.98800600
C	-1.32792200	-0.15722700	0.35991700
C	-0.29222800	-0.43587900	1.27382000
C	-2.08981600	0.43482900	-1.91600400
H	-1.84067800	0.68704000	-2.94166400
C	-3.38863700	0.31245600	-1.52972600
H	-4.19038700	0.46202900	-2.24445700
C	-3.70078300	-0.00127200	-0.17873900
H	-4.73815000	-0.06248000	0.12855500
C	-2.71057100	-0.22883800	0.72835500
H	-2.97796600	-0.46004700	1.75178000
C	-0.63944500	-0.89956100	2.66578800
H	0.19976000	-1.36888400	3.17289100
H	-1.43664400	-1.64466300	2.63841400
H	-0.98445900	-0.07511600	3.29859000

References:

1. Barnes, J. C.; Juricek, M.; Strutt, N. L.; Frasconi, M.; Sampath, S.; Giesener, M. A.; McGrier, P. L.; Bruns, C. J.; Stern, C. L.; Sarjeant, A. A.; Stoddart, J. F., ExBox: A Polycyclic Aromatic Hydrocarbon Scavenger. *J. Am. Chem. Soc.* **2013,** *135* (1), 183-192.
2. M. J. Frisch, G. W. Trucks, H. B. Schlegel, G. E. Scuseria, M. A. Robb, J. R. Cheeseman, G. Scalmani, V. Barone, B. Mennucci, G. A. Petersson, H. Nakatsuji, M. Caricato, X. Li, H. P. Hratchian, A. F. Izmaylov, J. Bloino, G. Zheng, J. L. Sonnenberg, M. Hada, M. Ehara, K. Toyota, R. Fukuda, J. Hasegawa, M. Ishida, T. Nakajima, Y. Honda, O. Kitao, H. Nakai, T. Vreven, J. A. Montgomery Jr., J. E. Peralta, F. Ogliaro, M. J. Bearpark, J. Heyd, E. N. Brothers, K. N. Kudin, V. N. Staroverov, R. Kobayashi, J. Normand, K. Raghavachari, A. P. Rendell, J. C. Burant, S. S. Iyengar, J. Tomasi, M. Cossi, N. Rega, N. J. Millam, M. Klene, J. E. Knox, J. B. Cross, V. Bakken, C. Adamo, J. Jaramillo, R. Gomperts, R. E. Stratmann, O. Yazyev, A. J. Austin, R. Cammi, C. Pomelli, J. W. Ochterski, R. L. Martin, K. Morokuma, V. G. Zakrzewski, G. A. Voth, P. Salvador, J. J. Dannenberg, S. Dapprich, A. D. Daniels, Ö. Farkas, J. B. Foresman, J. V. Ortiz, J. Cioslowski, D. J. Fox, Gaussian 09, Revision D.01. (Gaussian Inc., 2013)
3. Shen, L.; Zhang, H. Y.; Ji, H. F., Successful application of TD-DFT in transient absorption spectra assignment. *Org. Lett.* **2005,** *7* (2), 243-246.

4. Das, A.; Mandal, I.; Venkatramani, R.; Dasgupta, J., Ultrafast photoactivation of C-H bonds inside water-soluble nanocages. *Sci. Adv.* **2019,** *5* (2), 13.

5. Oyama, M.; Matsui, J., Kinetic analysis of the reactions of 1-substituted pyrene cation radicals with water in acetonitrile. *J. Electroanal. Chem.* **2004,** *570* (1), 77-82.

6. Young, R. M.; Dyar, S. M.; Barnes, J. C.; Juricek, M.; Stoddart, J. F.; Co, D. T.; Wasielewski, M. R., Ultrafast Conformational Dynamics of Electron Transfer in $ExBox^{4+}$ Perylene. *J. Phys. Chem. A* **2013,** *117* (47), 12438-12448